The Physics of Shock Wave Lithotripsy

Robin O. Cleveland, PhD
James A. McAteer, PhD

Shock wave lithotripsy (SWL) was introduced in the 1980s for the treatment of urinary stones and earned near-instantaneous acceptance as a first-line treatment option.[1] Since then SWL has revolutionized treatment in nephrolithiasis worldwide, and in the United States, it has been estimated that approximately 70% of kidney stones are treated using SWL.[2] Over the years, lithotripsy has undergone several waves of technological advancement, but with little change in the fundamentals of shock wave generation and delivery. That is, lithotriptors have changed in form and mode of operation from a user perspective—and in certain respects the changes have been dramatic—but the lithotriptor pressure pulse is still essentially the same. Lithotriptors produce a signature waveform, an acoustic shock wave. This pressure pulse, or shock wave, is responsible for breaking stones. However, it is also responsible for collateral tissue damage that in some cases can be significant.[3–6]

Lithotriptors produce a powerful acoustic field that results in two mechanical forces on stones and tissue: (1) direct stress associated with the high amplitude shock wave and (2) stresses and microjets associated with the growth and violent collapse of cavitation bubbles. Recent research has made significant advances in determining the mechanisms of shock wave action, but the story is by no means complete. What fuels this effort is the realization that a totally safe, yet effective lithotriptor has yet to be developed. Indeed, there is compelling evidence to suggest that a recent trend toward the development of lithotriptors that produce very high amplitude and tightly focused shock waves has led to increased adverse effects and higher re-treatment rates.[2,7–9]

A major objective within the lithotripsy community is to find ways to make SWL safer and more efficacious. The perfect lithotriptor may not exist, so urologists are left to determine how best to use the machines at hand. One step toward improving outcomes in SWL is to have a better understanding of how current machines work. Thus, the goal of this chapter is to introduce the basic physical concepts that underlie the mechanisms of shock wave action in SWL. Our aim is to give the background necessary to appreciate how the design features of a lithotriptor can affect its function. We also present a synopsis of current theories of shock wave action in stone breakage and tissue damage, and we summarize recent developments in lithotriptor technology. The main topics to be covered are as follows:

- Characteristics of a lithotriptor shock wave
- The acoustics of SWL
  - Acoustics primer
  - Acoustic cavitation
- The physics of clinical lithotriptors
  - Shock generation and shock focusing
  - Coupling the shock wave to the body
  - The focal zone of high acoustic pressure
- Mechanisms of shock wave action
  - How shock wave break stones
  - Mechanisms of tissue damage
- The evolution of the lithotriptor
- Future directions in lithotripsy

CHARACTERISTICS OF A LITHOTRIPTOR SHOCK WAVE

A typical shock wave measured at the focus of a lithotriptor is shown in Figure 38-1A. The wave is a short pulse of about 5 μs duration.* In this example, the wave begins with a near instantaneous jump to a peak positive pressure of about 40 MPa.† This fast transition in the waveform is referred to as a "shock." The transition is faster than can be measured and is less than 5 ns in duration.‡ The pressure then falls to zero about 1 μs later. There is then a region of negative pressure that lasts around 3 μs and has a peak negative pressure around –10 MPa. The amplitude of the negative pressure is always much less than the peak positive pressure, and the negative phase of the waveform generally does not have a shock in it—that is, there is no abrupt transition. The entire 5 μs pulse is generally referred to as a shock wave, shock pulse or pressure pulse—technically, however, it is only the sharp leading transition that is formally a shock.

Figure 38-1B shows the amplitude spectrum of the shock pulse (that is, it displays the different frequency components in the pulse). We see that a lithotriptor shock wave does not have a dominant frequency or tone, but rather its energy is spread over a very large frequency range—this is a characteristic feature of a short pulse. It can be seen that most of the energy in the shock wave is between 100 kHz and 1 MHz. This means that it is unlikely that a lithotriptor breaks kidney stones by exciting its resonance—as an opera singer might shatter a crystal glass.

The waveform shown in Figure 38-1A was measured in an electrohydraulic lithotriptor. A description of different types of shock wave generators is given below (see "The Physics of Clinical Lithotripsy"). Most lithotriptors produce a similarly shaped shock wave, but depending on the machine and the setting, the peak positive pressure typically varies between 30 and 110 MPa and the negative pressure between –5 and –15 MPa. In Figure 38-2A, we compare waveforms measured in an electrohydraulic lithotriptor and

*1 microsecond (μs) is 1 millionth of a second.
†1 megapascal (MPa) is about 10 atmospheres of pressure.
‡1 nanosecond (ns) is 1 billionth of a second.

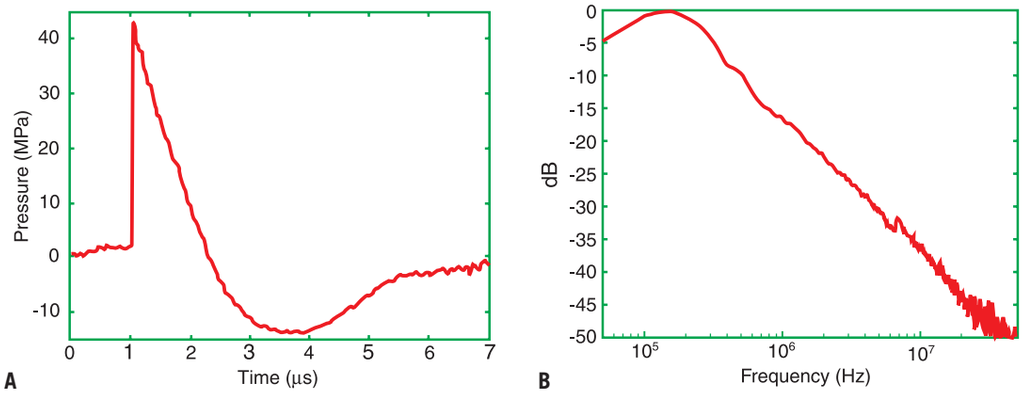

Figure 38-1 *A*, A pressure waveform measured at the focus of an electrohydraulic lithotriptor (Dornier HM3). *B*, The Fourier transform of the waveform in *A* showing how the energy is distributed as a function of frequency. (Both axes are shown on a log scale.) The peak of the amplitude response is around 300 kHz, which corresponds to the 4 μs duration. The energy between 1 MHz and 20 MHz can be attributed to the shock in the waveform. The steeper drop-off of energy for frequencies above 20 MHz is because that was the limit of the hydrophone for measuring the rise-time of the shock wave.

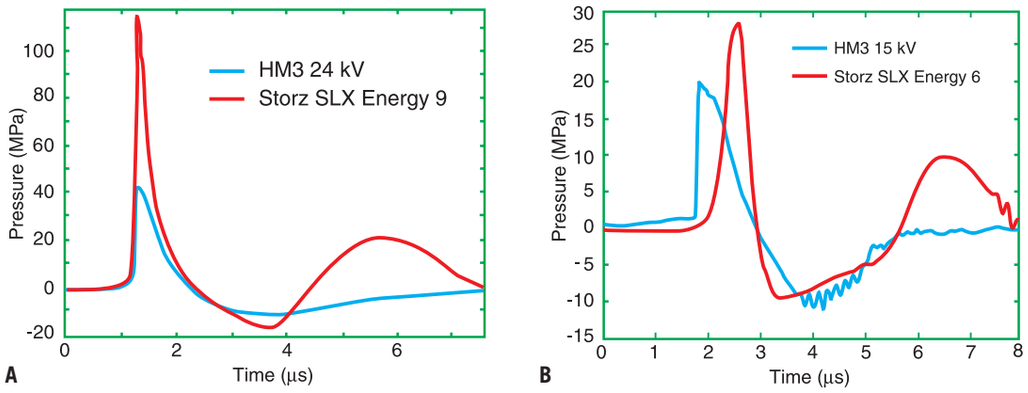

Figure 38-2 *A*, Focal waveforms measured in the Dornier HM3 at 24 kV and the Storz SLX at energy level 9. *B*, Comparison at lower settings—in this case the amplitudes are about the same, but the SLX waveform has not formed a shock.

an electromagnetic lithotriptor. It can be seen that the basic shape of both waveforms is very similar, consisting of a shock front, compressive phase, and tensile tail. For the settings chosen here, the main difference is the amplitude. Figure 38-2B shows waveforms measured at lower power settings of both machines, and again, the waveforms are similar, but the amplitudes are different.

Thus, lithotriptor shock waves show a unique form that contains a high amplitude, compressive phase of extremely rapid transition and short duration followed by a trailing tensile phase. The features of this waveform are similar regardless of the type of lithotriptor, but there are considerable differences in the amplitude and spatial extent of the acoustic output. It is likely that the amplitude and size of the focal zone of different lithotriptors affects their performance.

AN ACOUSTICS PRIMER FOR SWL

What is an Acoustic Wave? An acoustic wave, or sound wave, is created whenever an object moves within a fluid (a fluid can be either a gas or liquid). In Figure 38-3, we show that, as an object moves, it locally compresses the fluid that surrounds it—that is, the molecules are forced closer together. The compressed molecules in that region, in turn, push against the molecules next to them. This relieves the compression in the first region but leads to a new compressed region. The molecules in the second region then start to compress the next adjacent region, and so on; it is thus that a "wave" of compression travels through the fluid. This is an "acoustic wave," and the speed of wave propagation (called the sound-speed) is a material property of the medium. Note that individual molecules do not travel with the acoustic wave; rather, they just jostle their adjacent neighbors. Therefore, for an acoustic wave to propagate, there must be a medium present that can support the vibrations. This is an important physical difference between classical waves (eg, acoustic waves, seismic waves, water waves) and electromagnetic waves (eg, light, radio waves, x-rays). For electromagnetic waves, energy is carried by photons, which may be thought of as particles that physically travel through space; thus a medium is not needed for the signal to be transferred. Therefore, light can travel through a vacuum, but sound cannot.

Sound Waves Have Compressive and Tensile Phases The explanation above describes the compressive phase of a sound wave (that is, where the molecules are compressed). For the case where the object moves away from the fluid, there is a resulting rarefaction of the molecules (that is, the moving object leaves a partial vacuum). In this case, the neighboring molecules will move to fill the void, leaving a new region of rarefaction. This continues one region to the next, and the rarefactional disturbance propagates through the medium as a tensile acoustic wave. In most cases, a tensile wave propagates just like a compressive wave and with the same sound speed.

Typical acoustic sources, such as audio speakers, vibrate backwards and forwards. This produces alternating compression and rarefaction waves that are referred to as the compressive phase and tensile phase of the acoustic wave. Often the waveform is sinusoidal in nature. Note, however, that the majority of acoustic waves, including the acoustic pulses generated in lithotripsy, are not sinusoidal in form. For small-amplitude waves (linear acoustics), every point of the waveform moves at the same speed: the sound speed c_0. This is a material property, and for water and tissue, it is about 1,500 m/s. We will see later for large amplitude (nonlinear) acoustic waves, such as shock waves, that the sound speed is slightly changed by the presence of the wave.

The waveform shown in Figure 38-1 displays the pressure pulse as a function of time at a given point in space. This is typically how acoustic waves are measured; for example, a microphone will record how pressure varies in time at one point in space. Acoustic waves, however, also vary in space and it is often useful to think of the wave in terms of its spatial extent. The relationship between the temporal separation of points on an acoustic wave (Δt) and the spatial separation of the points (Δx) is related by:

$$\Delta x = \Delta t\, c_0 \qquad \text{(Equation 38-1)}$$

Recall that, in water or tissue, the sound speed is c_0 = 1,500 m/s = 1.5 mm/μs and therefore, for the shock wave shown in Figure 38-1, the positive part of the wave—a portion 1 μs long in time—will have a spatial extent in water of 1.5 mm. For a sinusoidal wave the spatial extent of one cycle of the wave is called the *wavelength*.

Sound Waves are not just Pressure Waves When a sound wave propagates, it affects the density, pressure, and particle velocity of the fluid particles. The impact on the density occurs because, as molecules are compressed together, the local density (ρ) will increase and in regions of rarefraction the density will decrease. For an acoustic wave it is convenient to write the total density as:

$$\rho = \rho_0 + \rho_a \qquad \text{(Equation 38-2)}$$

where ρ_0 is the ambient density of the medium (in the absence of sound) and ρ_a is the variation in the density due to the acoustic wave.

The pressure in the fluid can similarly be written as the sum of two terms:

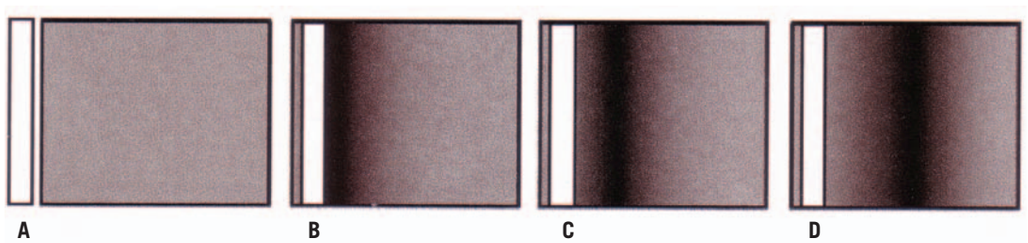

Figure 38-3 Illustration showing a molecular view point of a sound wave. *A*, Medium is at rest. *B*, A piston pushes all the molecules out of the left side, resulting in a localized region of compression at the face of the piston (dark region). *C*, The neighboring molecules are compressed and the compression region moves away from the piston. *D*, The wave continues to moved away from the piston. The molecules at the piston return to their ambient state.

$$p = p_0 + p_a \quad \text{(Equation 38-3)}$$

where p_0 is the ambient pressure (in the absence of sound) and p_a, the *acoustic pressure*, is the fluctuation due to the sound wave. For most fluids, acoustic pressure and density are directly related by an "equation of state" which takes the form:

$$p_a = \rho_a c_0^2 \quad \text{(Equation 38-4)}$$

That is, where the wave is compressed, the pressure will be positive, and where the fluid is rarefied, the pressure will be negative. Physically, pressure represents a force per unit area and has units of pascals (Pa). One pascal is quite a small pressure, and atmospheric pressure at sea level is approximately 100,000 Pa. In biomedical ultrasound, acoustic pressure is normally measured in megapascals (MPa).[§]

By way of example, the amplitude of the pressure from a diagnostic ultrasound scanner is about 2 MPa at the focus. Typically, values for ambient density and sound speed in tissue are $\rho_0 = 1{,}000$ kg/m^3 and $c_0 = 1{,}540$ m/s, and so this corresponds to a relative density perturbation of $\rho_a / \rho_0 = 0.0009$. For lithotripsy, peak pressures can be upwards of 100 MPa, which results in $\rho_a / \rho_0 = 0.04$. Therefore, the density disturbances associated with acoustic waves in medical devices—even the very strong waves that are produced in lithotripsy, actually result in very weak (less than 5%) compression of the fluid.

Progressive Waves and Particle Velocity The case shown in Figure 38-3, where the compression wave moves in one direction, is referred to as a *progressive wave*. In contrast, when there are sound waves traveling in different directions, this is referred to as a *compound wave*, which will not be considered here. For a progressive wave, the molecules in the compressed region also have a small net velocity away from the source. The net velocity of the molecules in a region of space is referred to as the *particle velocity* (u_a) and for a progressive acoustic wave it can be expressed as:

$$u_a = p_a / \rho_0 c_0 \quad \text{(Equation 38-5)}$$

Using the example of a 100 MPa shock wave, the instantaneous particle velocity at the peak is about 67 m/s. We will see below that the particle velocity is needed in order to determine the energy in an acoustic wave. It has also been suggested that the particle velocity within a biological target may produce sufficient strain to damage the cells.

Acoustic Impedance The density and sound speed of a material (Equation 38-4) determine its *specific acoustic impedance* ($Z_0 = \rho_0 c_0$). This term is often shortened to *acoustic impedance* or just *impedance*. The impedance of tissue and water is about 1.5×10^6 kg m^{-2} s^{-1}. The units are often referred to as Rayls—after the eminent nineteeth century acoustician Lord Rayleigh—although the Rayl is not an international standard.

Therefore, for a progressive acoustic wave, the pressure, density and particle velocity are not independent, but are linearly related to each other:

$$p_a = u_a Z_0 = \rho_a c_0^2 \quad \text{(Equation 38-6)}$$

where the coefficients are material properties. It follows that regions of high pressure are also compressed, and high particle velocity (away from source) and regions of low pressure are rarefied and have a negative particle velocity (towards the source). As the acoustic wave travels, the fluctuations in density, pressure, and particle velocity all move together (ie, "in phase"). Therefore, in a fluid with known material properties, if one property of an acoustic wave (such as the acoustic pressure) is measured, then Equation 38-5 can be used to determine the other acoustic properties.

Wave Intensity or Energy A propagating acoustic wave carries energy. The amount of acoustic energy per unit area is called the *energy flux, energy density, energy flux density*, or the *pulse intensity integral*. The IEC standard[10‖] calls this the "pulse intensity integral (energy density)" and it can be calculated by the following integral:

$$PII = \int p_a u_a dt \quad \text{(Equation 38-7)}$$

where the integration is done over the duration of the pulse. This is the acoustic equivalent to the expression from physics "work equals force times distance," where acoustic pressure is the force per unit area and the time integral of the velocity gives the distance.

The units for the pulse intensity integral (*PII*) are joules per square meter (J/m^2). For a progressive wave, we know that the particle velocity is related to the acoustic pressure $u_a = p_a/Z_0$ and therefore:

$$PII = \int \frac{p_a^2}{Z_0} dt \quad \text{(Equation 38-8)}$$

in which case, one only need measure the pressure of the wave to determine *PII*. Note that to calculate the integral, one needs to be able to accurately measure the entire pressure-versus-time waveform so that the integration can be done. The duration of a lithotripter pulse, for which this integral needs to be evaluated, is defined as the time from when the absolute value of the pressure first exceeds 10% of the peak pressure until the last time is exceeds 10% of the peak pressure.

To determine the energy in an acoustic wave, a specific area, A, has to be chosen, and the energy that passes through that area can then be calculated as:

$$E = \iint PII \, dA \quad \text{(Equation 38-9)}$$

where the double integral indicates a surface integral over the area A. The unit for energy is joules (J). The energy, E, will depend on both the size of the area A and how the intensity varies across the area. The *focal acoustic pulse energy* is calculated using the area in the focal plane, where the pressure is greater than half the maximum pressure (this is equivalent to the focal zone, see below). Energy can also be calculated over different areas, for example, the projected area of a stone or the area where the peak pressure is above 5 MPa.[11]

Another acoustic property used in the literature is the power per unit area, or the *intensity I*. Power is energy per unit time, and so the intensity is the energy density divided by the time over which the integration was done (Equation 38-8), which is normally the pulse length T_p:

$$I = \frac{PII}{T_p} \quad \text{(Equation 38-10)}$$

Intensity has units of watts per square meter (W/m^2) but it is more common in biomedical ultrasound to use centimeters (W/cm^2).

For a sinusoidal pressure wave the integral can be calculated exactly and the intensity is:

$$I = \frac{\hat{p}^2}{2Z_0} \quad \text{(Equation 38-11)}$$

where $\hat{p}$ is the peak pressure of the sinusoidal wave. If one substitutes the impedance for water or tissue (Z_0=1.5 MRayls) the relationship can be expressed as $\hat{p} = \sqrt{3I}$ where $\hat{p}$ is in atmospheres of pressure and I is in W/cm^2. For pulsed pressure waves, such as in lithotripsy, a simple expression does not exist for the intensity, as even small changes in the pulse shape can have a significant effect on the integration used to calculate *PII*.

Reflection and Transmission of Sound Waves When an acoustic wave encounters a medium with a different impedance, then part of the wave will continue to propagate into the new medium (the transmitted wave) and part of the wave will be reflected back into the original medium (the reflected wave). In the case of *normal incidence*, where the propagation direction of the shock wave is perpendicular to the surface, the amplitude of the transmitted and reflected waves depend only on the change in impedance between the two media, what is referred to as the *impedance mismatch*. In terms of acoustic pressure the transmission and reflection coefficients are:

$$R_p = \frac{Z_2 - Z_1}{Z_2 + Z_1} \quad \text{(Equation 38-12)}$$

[§]1 MPa is one million pascals, or approximately 10 atmospheres.

[‖]This standard describes how pressure measurements should be taken on a lithotriptor to ensure accurate results and fair comparisons across devices. The definition of terms used here is taken from the IEC standard.

$$T_p = \frac{2Z_2}{Z_2 + Z_1} \qquad \text{(Equation 38-13)}$$

There is a different set of coefficients for the intensity or energy, called the intensity transmission and reflection coefficients:

$$R_I = \frac{(Z_2 - Z_1)^2}{(Z_2 + Z_1)^2} = R_p^2 \qquad \text{(Equation 38-14)}$$

$$T_I = \frac{4Z_1Z_2}{(Z_2 + Z_1)^2} = 1 - R_I \qquad \text{(Equation 38-15)}$$

In Figure 38-4, we show the intensity transmission coefficient for an acoustic wave going from water to another medium with different impedance. We indicate typical values for tissue, kidney stones, bone, and air. One can see that the transmission from water to tissue is very efficient. The water-to-stone transmission is also relatively high, with 75 to 95% of the energy transmitted into the kidney stones. But a water-air interface has an extremely small coefficient, and less than 0.1% of the energy of an acoustic wave in water will pass into air—that is, 99.9% is reflected. This is why shock wave generators in lithotripsy are water-filled, why immersion of the patient in water gives the most efficient coupling of shock waves to the body, and why in dry lithotriptors, great care must be taken to eliminate air pockets between the shock head and the body. This is also one reason why stones are not targeted for treatment through lung or segments of gas-filled bowel. Indeed the best *acoustic window*, which allows the shock wave a pure tissue path to the kidney, is on the flank of the patient (delineated by the ribs, spine and pelvic bone).

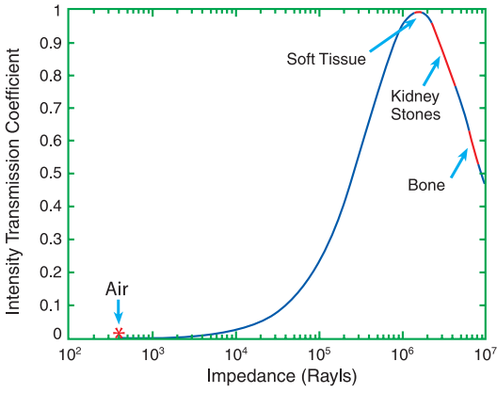

Figure 38-4 The intensity transmission coefficient (TI) from water ($Z = 1.5 \times 10^6$ Rayls) to a second medium, as a function of the impedance of the second medium. Typical values are indicated for soft tissue, kidney stones, bone and air. The transmission to soft tissue is very efficient. Coupling to air is very poor.

Focusing and Diffraction of Sound In lithotripsy, focusing of the shock waves is used to concentrate the acoustic energy onto the stone while reducing the impact on the surrounding tissue as much as possible. Lithotriptors achieve focusing by various means, including the use of reflectors, acoustic lenses, and spherically curved sources. Regardless of the method used, the physics that describes the focusing of the waves is similar for all these cases. An ideal focus would be the case where all energy is localized to an infinitesimally small region in space. However, the physics of wave propagation does not allow the energy to be focused to an arbitrarily small volume due to a process called *diffraction*. This means that, even though the acoustic pressure may be greatest at one point in space, there is a finite region or volume of surrounding space that is also at high amplitude. This is called the *focal zone*. For a theoretically optimal focusing arrangement, where sound can come in from all angles, diffraction puts a bound on the size of the focal zone of about one wavelength. For the realistic focusing arrangements used in lithotripsy, where the sound only comes from one direction, the focal zone can be from a few millimeters to tens of millimeters in size.

Focal zone The *focal zone* of a lithotriptor (equivalent terms include *focal region, hot spot, focal spot, focal volume, zone of high pressure*) is normally ellipsoidal in shape with its longest dimension along the axis of the shock wave. To demonstrate this, Figure 38-5 shows the predicted peak pressure of the focal zone in an unmodified Dornier HM3 lithotriptor.[12] The length and diameter of the focal zone depends on the diameter of the source, the focal length of the source, and the frequency content of the waveform. The dimension of the focal zone is thus one characteristic of any given lithotriptor that is determined by design features. Different lithotriptors have different focal zones and, as is discussed below, some lithotriptors generate extreme acoustic pressures delivered to a very narrow focal zone.

For a focused acoustic source that generates a sinusoidal waveform, such as an ultrasound transducer, there are analytical expressions for the size of the focal zone. The critical parameters are the wavelength of the sound wave (λ) and the half angle of the aperture:

$$\alpha = \arcsin(D/2F) \qquad \text{(Equation 38-16)}$$

where D is the diameter of the source and F the focal length. The formulae for the length (L_{FZ}) and the diameter (D_{FZ}) of the focal zone are:

$$L_{FZ} = \frac{0.6\lambda}{\sin^2(\alpha/2)} \qquad \text{(Equation 38-17)}$$

and

$$D_{FZ} = \frac{0.7\lambda}{\sin\alpha} \qquad \text{(Equation 38-18)}$$

Note that the focal length F is the distance from the mouth of the therapy head to the focus (where the stone should be placed). The focal length should not be confused with the length of the focal zone L_{FZ} which is the region around the focus where the pressure is high.

For a pulsed waveform, as is generated in lithotripsy, there are no explicit formulae for the size of the focal volume because the size depends on the waveform shape. But the focal region of a lithotriptor can be estimated using the formulae for the focal region of a sine wave. Figure 38-6A shows how the focal zone gets shorter and narrower as the diameter of the source aperture is increased. Figure 38-6B shows how the focal zone gets shorter and narrower as the focal length of the source (source-to-target distance) is decreased. Therefore, to make a small focal zone, a shock source with a large diameter aperture and short focal length would be desired. However, the size of the acoustic window in the flank and the need to be able to target stones deep in the body mean that, in most lithotriptors, both the focal

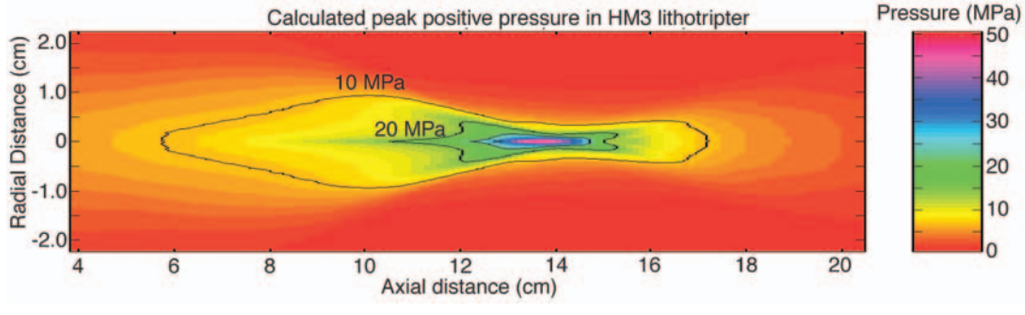

Figure 38-5 Predicted peak positive pressure in a Dornier HM3 lithotriptor. The pressure is not focused to a point but extends over a finite volume.

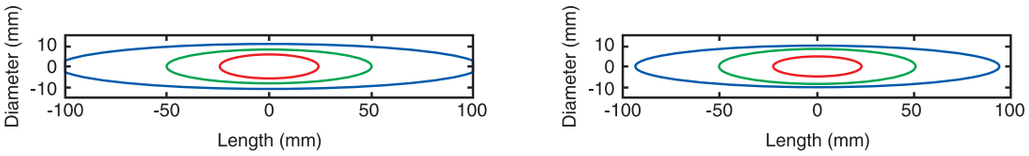

Figure 38-6 Predicted focal zone size as a function of the diameter of the source and the focal length of the source for a 500 kHz source. *A*, Contours show size of the focal zone for a source that has a focal length of 14 cm and with an aperture of 25 cm (red), 15 cm (green) and 10 cm (blue). The focal zone gets longer and wider as the aperture size decreases. *B*, Contours show the size of the focal zone for a source with fixed aperture diameter (15 cm) and varying focal length: 8 cm (red), 14 cm (green) and 20 cm (blue). The focal zone gets broader and longer as the focal length increases. For reference, the Dornier HM3 has focal length of 13 cm and an aperture diameter of 15 cm.

length and the diameter of the aperture are around 15 cm.

Nonlinear Acoustics When an acoustic wave has very large amplitude, for example a lithotriptor shock wave, the speed of the wave is no longer constant but depends on the local compression of the fluid. For "weak" shock waves (recall even at the focus of the highest power lithotriptor, the water is compressed by less than 5%) the speed of propagation ("phase speed") of an acoustic wave is:

$$c_{phase} = c_0 + \beta\, p_a / \rho_o\, c_0 \qquad \text{(Equation 38-19)}$$

where β is the *coefficient of nonlinearity* of the fluid and is a material property of the medium. For water, β is about 3.5, and for tissue, it varies from about 4 to 9. Normally, tissue of more complex structure has a greater coefficient of nonlinearity. A reasonable value for healthy soft tissue is $\beta = 5$.

Nonlinearity arises because of two physical processes; first, in regions of high pressure, the local sound speed is increased above the usual value; and second, the molecules in regions of high pressure have a higher particle velocity and are convected in the direction of acoustic propagation. For sound traveling through tissue, it is the first process that dominates the nonlinearity.

The difference between a nonlinear wave and a linear wave is that, for a nonlinear wave, different parts of the wave travel at different speeds as described by Equation 38-19. Figure 38-7 shows what happens to a sinusoidal wave as it propagates with nonlinearity present. The waveform becomes distorted in shape. In the absence of absorption, the wave obtains an infinite slope and then folds over and becomes multivalued. Ocean waves fanning up the beach are such waves, but this waveform is not physically realizable in acoustics—that is, it is not possible to have more than one pressure at any one point in space.

Shock formation The point at which the waveform first attains an infinite slope is called the shock formation distance. For a sinusoidal waveform the *shock formation distance* is:

$$\bar{x} = \frac{\rho_0 c_0^3}{\beta \hat{p} 2\pi f} \qquad \text{(Equation 38-20)}$$

Any acoustic wave can result in a shock wave if it can propagate for a long enough distance. For most sound waves encountered in everyday life, however, the shock formation distance is so long that the wave has been absorbed before it can form a shock. In lithotripsy the sound waves are intense enough that the wave typically does form a shock in the approximately 10 cm propagation path to the kidney.

Rise Time In acoustics, waveforms are prevented from folding over (or breaking) by the presence of acoustic loss mechanisms. All acoustic waves will leave behind a small fraction of their energy as they propagate through a fluid—this loss of energy is referred to as absorption. The absorption of sound is greater from waveforms with steep gradients. In the case of a shock wave where the slope tends towards infinity, the absorption will also tend towards infinity. The shock will, therefore, never attain an infinite slope, but instead, a balance between nonlinear distortion and absorption will result in a shock front where the pressure jumps in a very short time. This time is referred to as the *rise time* of the shock (or the Taylor shock thickness). For a shock wave in water, the expression for the Taylor shock thickness is:

$$T_{rt} = \frac{5}{\Delta P} \text{ns} \cdot \text{MPa} \qquad \text{(Equation 38-21)}$$

where ΔP is the pressure jump in MPa and the rise time (in ns) is defined as the time to go from 10% to 90% of ΔP. From this expression one finds that a 1 MPa shock should have a rise time of 5 ns and a 10 MPa shock a rise time of 0.5 ns. As a shock becomes stronger, the rise time shortens. Using Equation 38-1, one finds that the corresponding spatial extent of the rise time of the 1 MPa and 10 MPa shock waves is 7.5 μm and 0.75 μm, respectively.

Nonlinear acoustics phenomena are also important in other areas of biomedical ultrasound. In diagnostic ultrasound, nonlinear effects can create problems such as excess heating of tissue[13,14] but can also be beneficial by enhancing image quality in tissue harmonic imaging.[15–17] Nonlinear effects are also important in high intensity focused ultrasound surgery (HIFU or FUS), where ultrasonic heating of tissue is exploited to destroy specific regions of tissue or to coagulate blood (see ter Haar G,[18] Hynynen K,[19] Arefiev A,[20] and Bailey MR, et al[21]).

Absorption of Sound by Tissue As mentioned above, when a sound wave passes through a medium, most of the energy remains in the sound wave, but a small amount of it is absorbed by the medium. The amplitude of an acoustic wave will therefore slowly decay, or *attenuate*, as it propagates through a medium. The absorption in water is very low, and aside from controlling the rise time of the shock front, has little effect on lithotriptor waveforms. The absorption in tissue, however, is about 1,000 times larger than that in water and has a measurable effect on lithotriptor shock waves as they pass through the body and into the kidney. Typical values for absorption in muscle, fat and kidney are shown in Figure 38-8 as a function of frequency. One can see that the

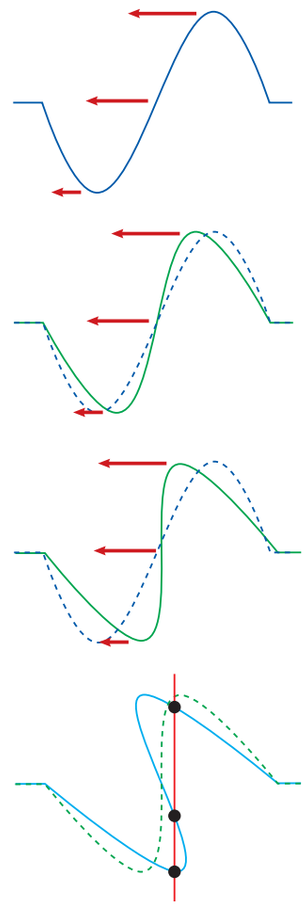

Figure 38-7 Nonlinear distortion of a sine wave based on Equation 38-19. *A*, Initial waveform; the length of the arrows shows the local phase speed of different points to the waveform. The peak will move the most quickly and the trough the least quickly. *B*, Waveform after a short amount of propagation (dashed line is waveform in *A*) showing how the shape has distorted. *C*, Shock formation distance where the slope of the waveform first becomes infinite (dashed line is waveform in *A*). *D*, Predicted multivalued waveform—the vertical line indicates that there are three different pressures predicted at one point in time (dashed line is from *C*). This shape is non-physical because absorption will prevent the wave from folding over.

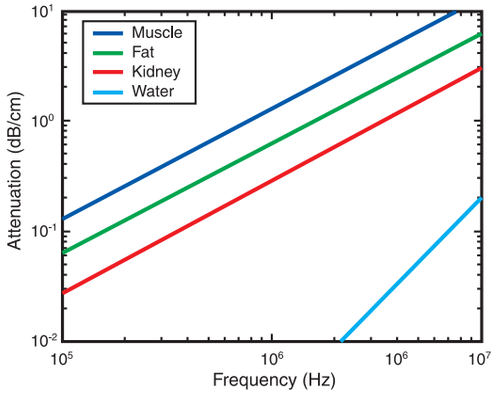

Figure 38-8 Attenuation of sound as a function of frequency for muscle, fat, and kidney tissue (listed in decreasing order of loss). Also shown is the attenuation in water, which is much less (1,000 times less at 1 MHz) than the attenuation of tissue.

absorption increases (almost linearly) with frequency. This means that energy is removed more effectively from the higher frequencies of the sound wave. In lithotripsy waveforms, the high frequency components are associated with the shock front. The primary action of tissue absorption is to increase the rise time of the shock front, and this will also result in the peak amplitude being reduced. The main energy components of the wave (which are around 500 kHz) will not be significantly impacted by tissue attenuation, and therefore, the basic shape of the pulse should not be affected by propagation through tissue, and the peak negative pressure, in particular, will not be sensitive to tissue absorption.

HOW SHOCK WAVES ARE MEASURED

Hydrophones Measure Shock Waves The main physical property of a lithotriptor is the spatial and temporal distribution of its acoustic pressure field. The acoustic field is typically measured in water using a hydrophone, which converts pressure into an electrical signal. Lithotriptors generate short (wide frequency band) high amplitude acoustic pulses, which are focused to a small volume in space. These physical parameters require that the hydrophone needs to (1) be very wide bandwidth (60 kHz to > 20 MHz), (2) be robust, to withstand the high pressures of the shock waves, and (3) possess a small active area ≈ 0.5 mm. The first reliable measurements of lithotripsy shock waves were performed with a hydrophone made of PVDF—a piezoelectric plastic.[22] PVDF has very wide bandwidth, is capable of measuring high amplitude acoustic pressures, and can be manufactured so that only a small region is active. Both membrane hydrophones and needle hydrophones have been used, however membrane hydrophones are considered to yield the best measurement of the shock wave.[23] One problem with PVDF is that the adhesion between water and PVDF is not strong and the tensile phase of the lithotripsy pulse can result in cavitation at the surface of the PVDF. This is a significant limitation that has two main consequences. First, it limits the ability of the hydrophone to measure the tensile phase of the shock wave because, once the bubble forms, the negative pressure is relieved and the hydrophone registers a pressure close to zero. Second, when the cavitation bubbles collapse, they can irreversibly damage the hydrophone.

Recently, a new hydrophone was developed—the fiber optic probe hydrophone (FOPH).[24] This is now considered to be the state-of-the-art for measuring lithotripsy shock waves and is the recommended device in the international measurement standard.[10] The FOPH consists of a laser that injects light into one end of an optical fiber; the other end of the fiber is placed in the lithotriptor field. The FOPH measures the light that is reflected from the end of the fiber and exploits the fact that the amplitude of the reflection depends on the pressure in the fluid. Several features make the FOPH superior to the PVDF membrane. Similar to PVDF, the FOPH has wide bandwidth and is capable of measuring very high pressure amplitudes. The diameter of the active area of the FOPH (100 μm) is smaller than most PVDF hydrophones (500 μm). Also, the FOPH is made of an optical fiber (silica), and the adhesion between water and silica is very high. This means that cavitation is much less likely to occur at the surface of the FOPH, and therefore, it can more accurately capture the tensile phase of the shock wave. This also means that the FOPH is less susceptible to damage from cavitation. The main drawback with the FOPH is that the signal it generates is weak and therefore not good for measuring low pressures (≈2 MPa and less).

Measuring Shock Waves in the Body All published measures of dimensions of the focal zone come from in vitro experiments, and there have been few attempts to collect any shock wave pressure data within animals. Both the high attenuation and inhomogeneous nature of tissue will affect shock waves as they propagate through the body. Figure 38-9 shows representative pressure waveforms for a Dornier HM3 measured in water and for a PVDF membrane hydrophone implanted in a pig.[25] The in vivo waveform is very similar in basic shape to the in vitro waveform. The main difference is that the in vivo waveform has a 30% decrease in peak positive pressure and a greatly increased shock rise time (70 ns). Both of these effects are consistent with the higher attenuation associated with tissue.

What is Acoustic Cavitation? A second mechanical force generated by lithotriptor shock waves is *acoustic cavitation*. This refers to the generation of cavities in a fluid (ie, bubbles) when the tensile phase (negative pressure) of the acoustic wave is sufficiently strong to rip the fluid apart. In lithotripsy, the tensile phase of the shock wave is large enough (≈10 MPa) to generate violent cavitation events. Cavitation is believed to play a significant role in tissue damage during SWL and to contribute to stone comminution.[26–28]

Typically, cavitation is initiated at micron size motes in the fluid or at sites of small gas pockets trapped on rough surfaces.[29] There are a number of different theories available[30,31] that can describe how acoustic cavitation proceeds once the cavity has been formed—at this point, the cavity is normally referred to as a bubble. In Figure 38-10, we show the predicted radius of a spherical bubble as a function of time in response to a lithotriptor shock wave. The bubble is first compressed by the positive phase of the shock wave. Then the tensile phase of the shock wave causes the bubble to grow from 1 μm radius to about 1 mm radius over a period of 150 μs. Note that the bubble continues to grow long after the shock wave has passed (5 μs time frame), and this is referred to as inertial cavitation as the dynamics of the bubble are no longer driven by acoustics, but instead, by the inertia of the fluid surrounding the bubble. While the bubble is large, some amount of gas and vapor from the fluid will diffuse into the bubble. The bubble will then collapse by virtue of the near vacuum inside the bubble and the roughly 1 atmosphere of ambient pressure in the surrounding fluid. It takes a further 150 μs for the bubble to collapse. The collapse is very violent, and the gas that diffused inside is heated and compressed to such an extent that it can produce light.[32] The main collapse is followed by rebounds, after which the gas that had diffused into the bubble will slowly diffuse back out into the fluid. Also shown in Figure 38-10, is the acoustic emission radiated by the bubble; a lithotripsy-induced cavitation bubble

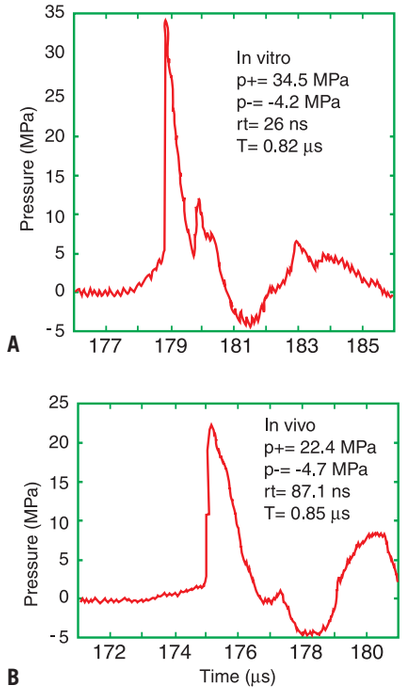

Figure 38-9 *A*, Waveform measured in water with a miniature PVDF hydrophone in a Dornier HM3 at 18 kV. *B*, Waveform measured in vivo in a pig for the same settings. The peak amplitude in vivo was about 30% less than that in water, and the rise time in vivo (87 ns) was much longer than that measured in water (26 ns).

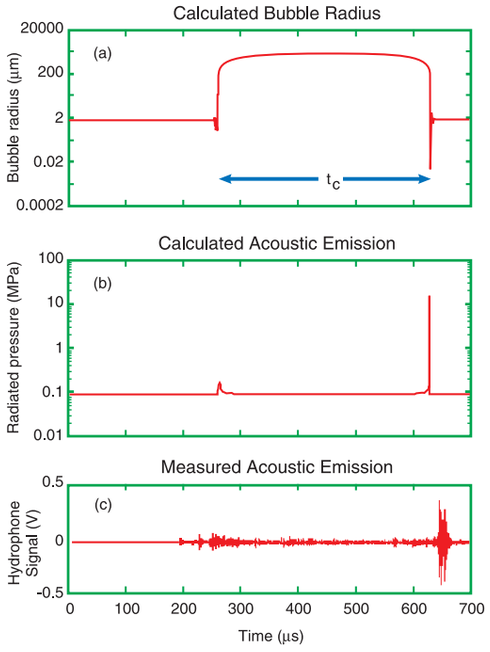

Figure 38-10 *A*, Calculated radius versus time curve of a spherical bubble subject to a lithotriptor pulse (as in Figure 38-1). In this time scale, the shock wave arrives at the focus at 250 μs, and the bubble is initially crushed by the leading compressive phase. The bubble grows to a millimeter-size bubble at about 450 μs. It then starts to collapse, with a violent collapse occurring at 650 μs. The time between the two collapse signals is the characteristic time t_C. *B*, The predicted acoustic emissions that the bubble calculated in *A* will radiate. There are two emissions due to the two collapses. *C*, Measured acoustic emissions in a Dornier HM3 using a PCD (see Figure 38-11). The measured emissions agree with the calculations.

generates two acoustic emissions, one when it is hit by the compressive wave, and one when it collapses hundreds of microseconds later. This unique "double-bang" signature can be used to detect the cavitation events.[32]

There are numerous techniques by which cavitation can be measured.

High-Speed Photography Bubble behavior can be observed using a high-speed camera in an in vitro setting.[33–36] In principle, this allows the entire dynamics of a bubble to be tracked from genesis to extinction. In practice, this is not feasible. During the growth phase, the bubble needs to be imaged at millimeter-length scales and tens of microseconds time scales. At the nadir of the collapse, the bubble radius is less then a 1 μm, and the dynamics of the collapse is at nanosecond time scales. The remnant bubble left after the rebounds, is on order of 10 μm and slowly dissolves over hundreds of milliseconds. Thus, the range of temporal and spatial scales makes it virtually impossible to capture all the bubble dynamics photographically. Therefore, investigators have found it necessary to study cavitation in segments. A further limitation of imaging is that cameras have a limited depth of field and cannot give an adequate record of bubble dynamics throughout the substantial volume of the cavitation field.

Laser Scattering of Single Bubbles The dynamics of a single spherical bubble can be measured very precisely by laser scattering.[37] In this case, a laser beam is used to illuminate a bubble, and a photodetector is used to collect the light scattered by the bubble. For a spherical bubble, the amplitude of the scattered light varies in a known way as the bubble radius changes. This method is able to capture most of the temporal and spatial scales associated with the dynamics of a lithotripsy-excited cavitation bubble. But laser scattering has several restrictions: the sample volume is very small, the method requires unrestricted visual access at high magnification, and the theory that is used to recover the actual bubble size is based on a single spherical bubble. This means the technique will only yield qualitative information about bubble clouds or nonspherical bubbles, both of which are very common in lithotripsy induced cavitation.

Acoustic Detection Can Be Used In Vivo Acoustic detection of bubbles is very powerful, in part, because it can be used to characterize bubble dynamics within living subjects. Acoustic detection normally works in one of two modes: active cavitation detection (ACD) and passive cavitation detection (PCD).[38–40] In ACD, one transducer is used to send an acoustic wave toward the cavitation field, while a second transducer picks up sound reflections from the bubbles—this is the acoustic analogue to laser scattering. In PCD, one or more receiving transducers listen for the "double-bang" acoustic emissions from cavitation bubbles. In the case where two receiving transducers (dual PCD) are used, it is possible to take advantage of coincidence detection to sample a small, discrete volume of the cavitation field where the transducers intersect.[41] The timing and amplitude of the two emissions is influenced by various factors, such as the size of the initial bubble and the amplitude of the lithotriptor pulse. Thus, although acoustic detection does not image bubbles (that is, it cannot provide information on bubble number and size) it gives valuable data that can be used to help characterize the acoustic output of a lithotriptor and assess the environment and dynamics of the cavitation field.[35,41,42]

Other techniques have also been developed for measuring cavitation (Figure 38-11). It has been observed that cavitation leads to pitting on metal foils, and the number and depth of pits can be used to assess the violence of cavitation.[26,43,44] An electromagnetic probe device has been used to measure the mechanical force exerted on a steel ball by both the incident shock wave and the cavitation activity.[45] The high pressures and temperatures in the interior of the bubble provide an environment that can produce light emissions (sonoluminescence) and also result in enhanced chemical reaction rates (sonochemistry). Production of light and byproducts from chemical reactions have both been used to quantify cavitation activity.[37,42] These are secondary measurements of the cavitation field, and interpreting the results in terms of physical processes can be complicated.

THE PHYSICS OF CLINICAL LITHOTRIPSY

Shock Generation and Focusing Three shock wave generating principles have been used in clinical lithotriptors.

Electrohydraulic Lithotriptors The electrohydraulic lithotriptor (EHL) has a spark source, which generates a shock wave that is focused by an ellipsoidal reflector (Figure 38-12). In an EHL, the pressure pulse originates as a shock wave and remains a shock wave at all times during its propagation from the spark source to the reflector, and then as it focuses to the target. As we will see below, this is not the case for other types of shock wave sources. In an EHL, focusing of the shock wave is critically dependent on the placement of the spark at the first focus of the ellipse. Misalignment by just a few millimeters can lead to a significant loss in focusing and a lengthening and broadening of the focal zone. Thus, EHLs are designed so that the

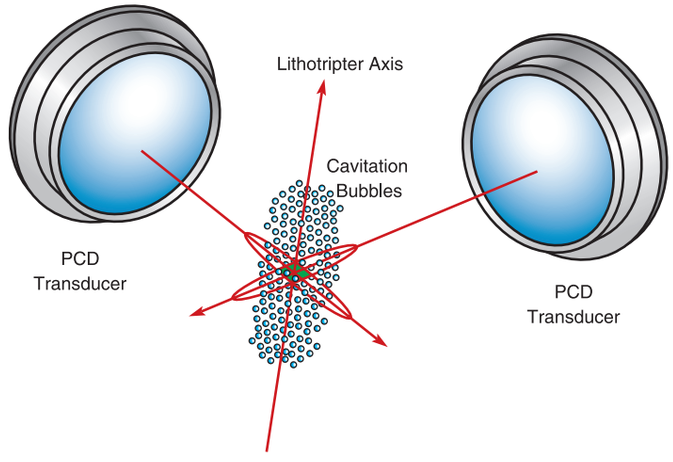

Figure 38-11 Schematic showing the dual passive cavitation detection system. Two focused transducers are placed so that their ellipsoidal focal zones intersect. Acoustic emissions that occur in the shaded region of intersection can be localized by searching for simultaneous events on both transducers.

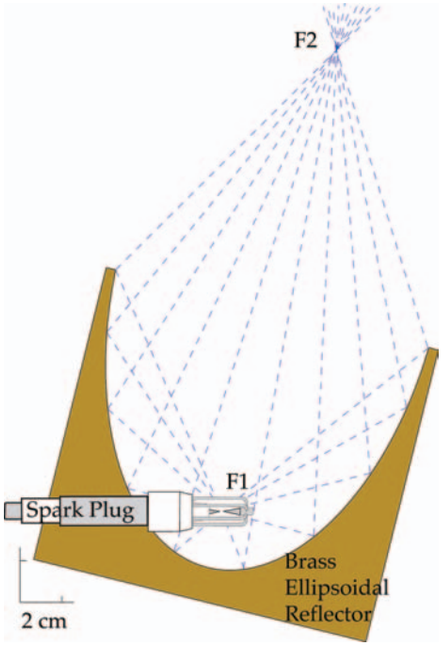

Figure 38-12 The focusing design of a Dornier HM3 electrohydraulic lithotriptor. A spark plug is located at the focus (F1) of an ellipsoidal reflector. Energy from the spark plug is reflected and focused to the second focus of the ellipsoidal reflector (F2).

alignment of the electrode is consistent. Still, there is variability of the precise location of the spark discharge across the spark gap that is not easy to control. Therefore, from shot-to-shot, there can be significant variation (upwards of 50%) in the amplitude of the shock wave, and there can be some shift in the position of the focal zone at the target. A unique "feature" of EHLs is that the target is insonified by two pulses. The main focused pulse is preceded by the so-called "direct wave," which travels directly from the spark to the target without bouncing off the reflector. The direct wave arrives about 30 μs earlier and because it undergoes spherical spreading it is low in amplitude. However, it has been shown that this direct wave can influence the cavitation generated by the focussed wave.

In EHL, the electrodes wear out and must be replaced. Some lithotriptor manufacturers have found ways to enhance the lifetime of their electrodes, such as by encapsulating them and filling the casing with an appropriate electrolyte. Still, electrodes eventually show wear and this can affect their acoustic output.

Electromagnetic Lithotriptors The electromagnetic lithotriptor (EML) uses an electrical coil in close proximity to a metal plate as an acoustic source. When the coil is excited by a short electrical pulse, the plate experiences a repulsive force and this is used to generate an acoustic wave. If the metal plate is flat, the resulting acoustic wave is a plane wave that can be focused by an acoustic lens (Figure 38-13A). If the plate is in the shape of a tube, the resulting cylindrical wave can be focused by a parabolic reflector (Figure 38-13B). In both cases, focusing is very reproducible, and the variation in measured pressure waves is less than 10%. Thus, the shock waves generated by electromagnetic lithotriptors are inherently more consistent than in EHL. An additional advantage is that there are no electrodes to replace.

One difference between the acoustics of an EML and an EHL is that the acoustic pulse generated by an EML does not start as a shock wave; the displacement of the plate generates a high-intensity ultrasonic wave, which has a smooth waveform with no discontinuities. The amplitude of the wave at clinically relevant power settings is normally high enough that nonlinear distortion occurs during propagation, and a shock is produced before the wave reaches the focus. A second difference is that the EML waveforms have a relatively small trailing positive pressure after the negative phase. This peak likely has little impact on the stress inside the stone but may affect the cavitation dynamics.

Piezoelectric Lithotriptor The piezoelectric lithotriptor (PEL) uses piezoelectric crystals to form an ultrasonic wave. When a voltage is applied to a piezoelectric crystal it deforms and creates an acoustic wave. The crystals are placed on the inside of a spherical cap and the acoustic wave focuses at the centre of the curvature of the sphere, (Figure 38-14A). This focus is highly reproducible, and very small variations in the focal waveforms are reported. Similar to the EML, the acoustic waveform in the PEL starts as an acoustic pulse, and a shock wave is created by nonlinear propagation distortion. For most clinical settings, a shock is produced before the wave reaches the focus. Figure 38-14B shows a representative waveform from a piezoelectric lithotriptor.[46] Also similar to the EML is the presence of a tail, or coda, at the end of the pulse. The coda is much more pronounced for a PEL. This is because the piezoelectric crystals "ring" for a couple of cycles after they are excited—a phenomenon not present in an EHL or EML. As with the EML, the PEL coda should not affect the stress in the stone but may affect the cavitation.

Coupling of the Shock Source to the Body

Efficient transfer of acoustic energy from one medium to another only occurs when the acoustic impedances are very close. A water/tissue interface results in very good coupling, and theoretically, it should be possible to transfer more than

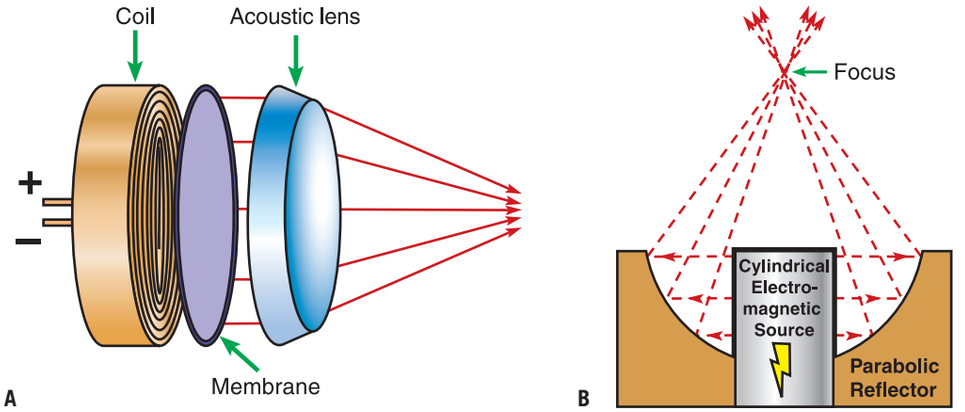

Figure 38-13 The two focusing mechanisms employed in electromagnetic lithotriptors. *A*, In a Siemens or Dornier lithotriptor, a membrane is driven by a coil to produce a plane wave, which is then focused by an acoustic lens. *B*, In a Storz lithotriptor, a coil excites a cylindrical membrane, which generates a wave that is focused by a parabolic reflector.

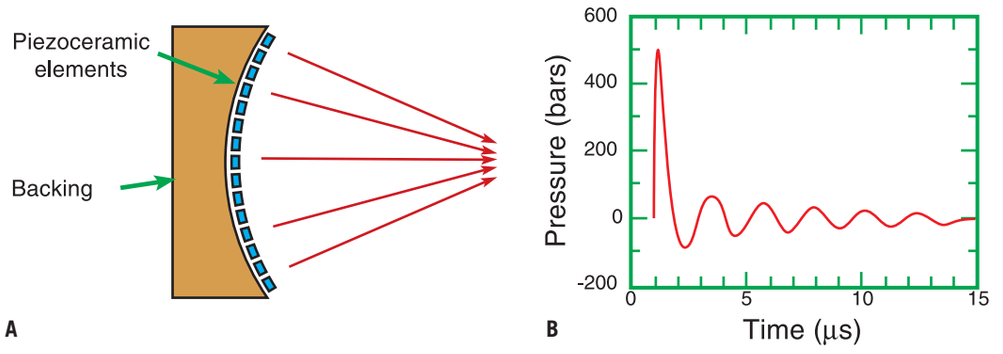

Figure 38-14 *A*, Fundamental principles for a piezoelectric lithotriptor. Piezoceramic elements are placed onto the surface of a sphere. The wave will focus to the center of the radius of curvature of that sphere. *B*, A typical waveform measured at the focus of a piezoelectric lithotriptor—notice the long ring-down for time greater than 3 μs.

99% of the energy of the shock wave into the body. But the presence of even a small pocket of air at the skin surface will result in a dramatic reduction in energy transfer to the patient (see Figure 38-4). Thus, the manner in which the shock wave is coupled to the body is critical.

Water-Bath Lithotriptors The "first-generation" lithotriptors (eg, the Dornier HM3) were electrohydraulic lithotriptors and used an open water bath in which the patient was immersed. Thus, there was nothing but water between the shock source and the patient. This is ideal except that the bubbles that drift up from the spark-gap, or the cavitation bubbles that form along the path of the shock wave, have the potential to collect against the skin of the patient and interfere with the propagation of subsequent shock waves. To help prevent this, the ellipsoidal reflector of the shock source is fixed off vertical—in the Dornier HM3 the angle is 14 degrees—and the water in the bath is continuously degassed.

Dry Lithotriptors Most current lithotriptors have the shock wave source mounted in a "therapy head," which is filled with water. The therapy head is capped by a thin rubber membrane pressed against the patient and through which the shock wave passes. A coupling agent such as gel or oil is smoothed on the rubber membrane and the patient's skin to ensure good coupling by reducing air pockets. The water in the therapy head of most lithotriptors is continuously recirculated and degassed to remove any bubbles that might interfere with the shock wave propagation. Although this design is more convenient in the clinic than a water–bath-type of lithotriptor, it is inherently less effective at allowing shock waves to pass because the presence of the rubber (although well-matched to water and tissue) adds additional reflecting interfaces. Further, even with the application of a couplant, the presence of small air bubbles between the skin and membrane is almost impossible to avoid. In vitro experiments have shown that the type of couplant can have a significant effect on stone breakage.[47] At present, the convenience of a dry therapy head appears to outweigh performance issues.

The Focal Zone of the Lithotriptor In lithotripsy, acoustic energy is focused to a relatively small zone surrounding the *focal point* of the lithotriptor. The focal point is a geometric point in space (eg, in an EHL, this point is the second focal point [F2] of the ellipsoidal reflector) and is usually the location of the stone for treatment. All extracorporeal lithotriptors have a focal point, but lithotriptors differ in the dimensions of the zone of high pressure (*focal zone)* that surrounds this point. The dimensions and the pressure characteristics of the focal zone are the most important features that distinguish one lithotriptor from another.

There are many definitions of the focal zone that may be appropriate for lithotripsy. The IEC standard for measuring lithotriptor pulses[10] defines it as the volume within which the measured peak acoustic pressure is at least half the maximum peak positive pressure. The peak positive pressure (p+) of a waveform (see Figure 38-1) is the highest positive pressure in that waveform. The maximum peak positive pressure is the highest value of p+ in the field of the lithotriptor, and the location of the maximum peak positive pressure is defined as the focus.[10] The maximum peak pressure will vary with the power of the machine. The resulting focal zone is normally an elongated, elliptical "cigar-shaped" volume. It is worth noting that maximum peak pressure does not necessarily occur at the location the manufacturer will indicate a stone should be placed, and the location of the focus and the dimensions of the focal zone may change as the power setting is changed.

The Dornier HM3 has been used clinically more than any other lithotriptor and has been studied and characterized more extensively than any other lithotriptor. As such, data for the Dornier HM3 prove to be a useful standard for reference. Because different lithotriptors, even the same type of lithotriptor, may perform somewhat differently, and because investigators have used different means to map the acoustic field of their lithotriptors, published values for peak pressures and dimensions of the focal zone of a given type of lithotriptor may not coincide perfectly. Representative focal zones of selected lithotriptors are shown in Figure 38-15. Typical published values for the Dornier HM3 electrohydraulic lithotriptor report the maximum peak positive pressure to be 40 MPa at 20 kV and the focal zone to be about 60 mm long by 12 mm in diameter. In contrast. the Storz Modulith electromagnetic lithotriptor has a maximum peak positive pressure around 100 MPa at energy level 8 and a focal zone that is about 35 mm long and only 4 mm in diameter. Reported values for piezoelectric lithotriptors indicate a maximum peak positive pressure of 80 MPa and a focal zone 20 mm long and 3 mm in diameter.[48,49] Thus, there is a considerable difference in the dimensions of the focal zone between lithotriptors, and typically lithotriptors with narrower focal zones have higher peak pressures.

The half-maximum focal zone (also known as –6 dB focal zone because the contour corresponds to the pressure being 6 decibels less than at the maximum) is recommended in the IEC standard, but this may not necessarily be the best descriptor of the focal zone of a lithotriptor. For example, in a Storz lithotriptor, with a peak pressure of 110 MPa at energy level 9, the focal zone will correspond to a surface where the peak pressure is 55 MPa. For an Dornier HM3, which only has a peak pressure of 40 MPa, the focal zone will correspond to a surface where the pressure is just 20 MPa. Therefore, when comparing the focal zones of these machines, the absolute pressure levels are very different—indeed the focal zone of a Dornier HM3 would be zero if the 55 MPa level of the Storz focal zone were used. Other suggestions for the focal zone include: (1) half the peak negative pressure, (2) half the energy density, (3) the surface where the peak pressure is 5 MPa, or (4) even using the energy that passes through a volume with diameter 10 mm (about the size of a typical stone). Until there is a better understanding of how shock waves fragment stones, it is unlikely that an alternative metric will be agreed upon within the literature.

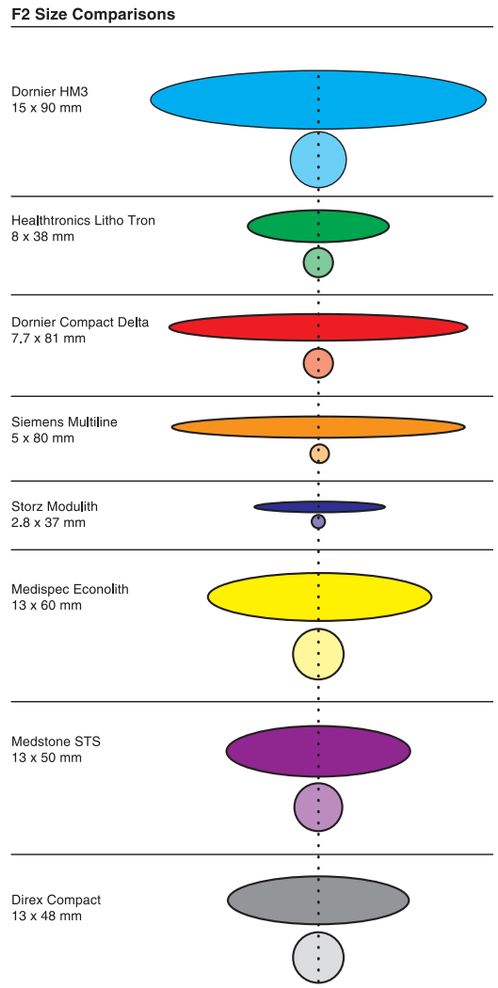

Figure 38-15 Comparison of the focal zones of selected clinical lithotriptors showing their dimensions along the axis of the lithotriptor (ellipses) and in the focal plane at the focus (circles). Image courtesy of P. Blomgren.

The smaller, tighter, focal spot of an electromagnetic or piezoelectric lithotriptor would at first glance appear to be advantageous because it should allow for more accurate targeting on the stone, and thus, less damage to the surrounding tissue. But in vitro experiments (where stones are stationary) indicate that the electromagnetic or piezoelectric lithotriptors, with their very high pressures, are no better at breaking stones that an electrohydraulic lithotriptor and often are not as effective.[50,51] High peak positive pressure does not appear to correlate with enhanced stone fragmentation in the clinic.[2]

Further, stone motion due to respiration means that, with a tight focal zone, fewer shock waves actually hit the stone, and more shock wave energy is deposited directly into tissue.[52] When one considers that some tight focal zone lithotriptors have peak pressures in excess of

100 MPa, this suggests that tissue is being subjected to a very high dose of acoustic energy. This may help explain the increased incidence of adverse effects, such as subcapsular hematomas observed with these machines.[3,8]

Device Equivalency/Equating Lithotriptor Performance At present, there are no agreed metrics by which the acoustic output of different lithotriptors can be compared, and there is no straightforward means to operate any given lithotriptor so that it is equivalent to another. This is partly due to the fact that, although all lithotriptors produce shock waves that have similar waveforms, the amplitude and focal zone of different lithotriptors is not the same, and measurements of the properties of the acoustic field can yield very different values. This is illustrated in Table 38-1, where we show a number of physical measurements made on an electrohydraulic and an electromagnetic lithotriptor.[53] For the settings chosen, the only parameter that was roughly equivalent was the energy incident on a 6.5 mm diameter stone (0.484 mJ versus 0.528 mJ). Other physical measurements, however, varied tremendously; for example, the peak positive pressure in the electromagnetic lithotriptor was three times that of the electrohydraulic lithotriptor.

Therefore, although it is possible to find settings on two given machines that give equivalency on one physical property, it is unlikely that there will be equivalency on other properties, and indeed, there are likely to be significant differences. For example, if the power setting were to be reduced on the electromagnetic lithotriptor to yield the same pressure as the electrohydraulic lithotriptor, then the energy measurements would drop by almost a factor of 10.

A further confounding issue is the number of shock waves to be used. The clinical literature suggests that typically fewer shock waves are required to break stones with an electrohydraulic device than with an electromagnetic device. In addition, the rate at which shock waves are delivered has also been reported to affect fragmentation efficiency.[54] Therefore, at the current time, there is no clear way in which the three main parameters of shock wave delivery for a lithotriptor (power, number of shock waves and rate of shock wave delivery) can be adjusted to ensure equivalency between different machines.

MECHANISMS OF SHOCK WAVE ACTION

Waves in Stones The acoustic field in stones is more complex than the acoustic theory described above. Kidney stones are elastic solids and support two types of waves: a longitudinal or compression wave (which is akin to an acoustic wave) and transverse of shear waves, where the motion of the vibration is transverse to the direction of propagation. In a shear wave, the transverse vibration does not result in the molecules being compressed and rarefied, but rather they oscillate in a manner analogous to the wave motion of a rope excited by a snap of the wrist. Longitudinal waves and shear

Table 38-1 Comparison of Physical Properties Measured in an Electrohydraulic Lithotriptor (EHL) and an Electromagnetic Lithotriptor (EML)

	L_{FZ}	W_{FZ}	p+	p-	E_{FZ}	E_{STONE}	t_C
EHL	54 mm	9 mm	37.5 MPa	-7.8 MPa	4.25 mJ	0.484 mJ	250 µs
EML	32 mm	3.5 mm	115 MPa	-14.6 MPa	3.35 mJ	0.528 mJ	350 µs
Ratio EH/EM	1.69	2.57	0.33	0.53	1.27	0.92	0.71

The columns show measurements of the length (L_{FZ}) and width (W_{FZ}) of the focal zone, the peak pressures (p+ and p-), the energy in the focal zone (EFZ) (Equation 38-9 using the area given by the width of the focal zone), the energy incident on a stone (E_{STONE}) (Equation 38-9 using the area given by the 6.5 mm diameter of the stone), and the characteristic time of cavitation (tc), which is a measure of the strength of cavitation. The bottom row shows the ratio of the values in the EHL to the EML. For the settings used here, the energy delivered to the stone was the one quantitative parameter that was approximately equivalent. Adapted from Chitnis PV.[53]

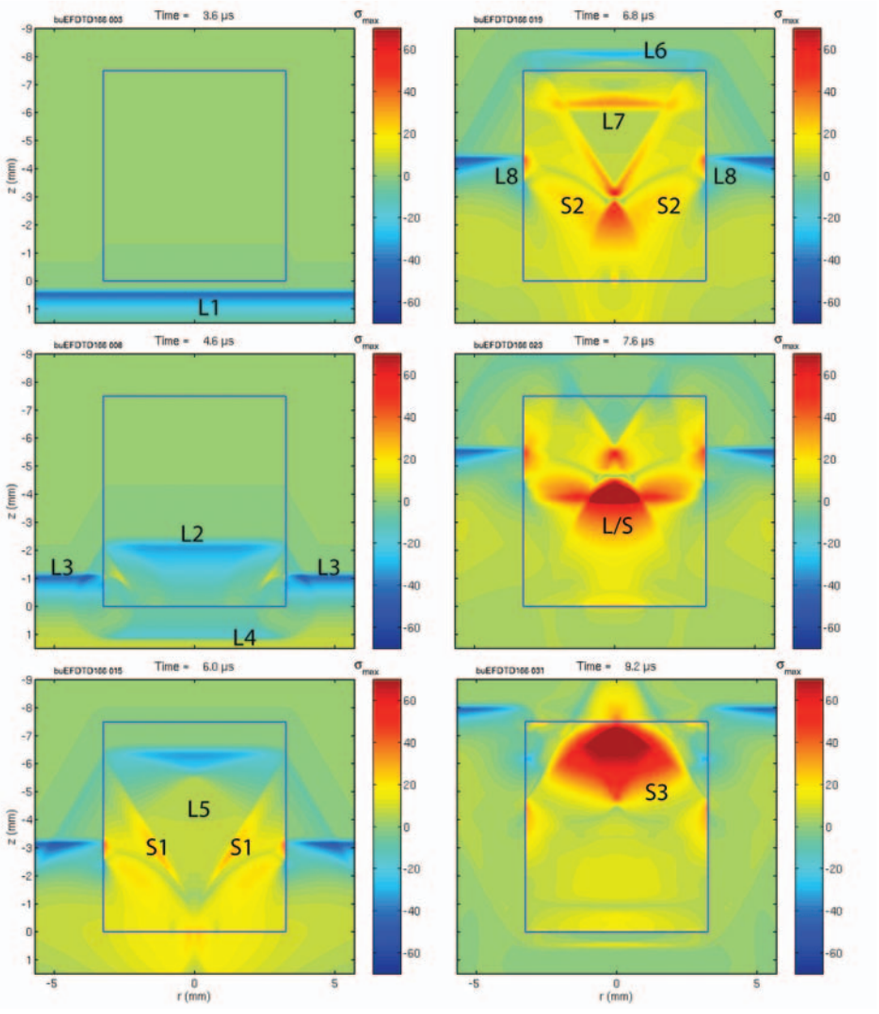

Figure 38-16 Snap-shots of the tensile stress generated by the propagation of a lithotripsy shock wave through a model kidney stone surrounded by fluid. The cylindrical stone (6.5 mm wide by 7.5 mm high) has the following properties p=1700 kg/m3, c_T=3000 m/s c_S=1500 m/s. The shock wave is incident from below and colour scale depicts the tensile stress (in MPa) where yellow through red indicate regions of tensile stress and blue regions of compression. In the first frame (3.6 µs) the leading compressional phase of the shock wave in the fluid (L1) is almost incident on the proximal surface of the stone. At 4.6 µs the shock wave has entered the stone as a longitudinal wave (L2), note because the propagation axis is normal to the surface no shear waves are generated at this interface. Because the speed in the stone is higher than in the fluid, the wave in the stone advances ahead of the wave in the fluid (L3). The reflection of the shock wave by the proximal surface can be seen leaving the bottom of the image (L4). At 6.0 µs the tensile tail of the incident shock wave can be seen in the stone (L5) following the leading compressive phase. The interaction of the longitudinal wave in the stone with the lateral walls of the stone results in the production of shear waves (S1)that propagate towards the axis of the stone. At 6.8 µs the leading compressive phase has been partially transmitted (L6) and reflected (L7) at the distal surface. The reflection coefficient is approximately -0.5 and results in a tensile phase (L7) that generates significant tensile stress (red region) near the distal surface—this is spall. The wave on the outside of the stone (L8) is inducing further shear waves (S2) inside the stone. At 7.6 µs the reflected longitudinal wave and the shear waves interact to produce a large region of tensile stress in the centre of the stone (L/S). At 9.2 µs the shear waves interact near the distal surface to generate another region of high tensile stress (S3).

waves travel at different speed and the longitudinal wave speed (cL) is always faster than the transverse wave speed (cT).

When a shock wave passes from urine or tissue into a stone the transmitted energy is divided between the longitudinal and transverse waves in the stone. The proportion of the energy that each wave gets depends on the material properties of the stone and the angle of incidence. If the wave is normally incident on the stone surface then all the energy is converted into a longitudinal wave in the stone and no energy is available for transverse waves. As the angle of incidence increases less energy is converted into a longitudinal wave and more is converted into transverse waves. The complex shape of many natural stones results in a non-trivial partition of energy between the two types of wave.

The basic features of the interaction of shock waves with a stone can be illustrated by means of a computer simulation. The computer simulation solves the equations of motion for particles in an elastic solid.[55] Figure 38-16 shows a series of snap-shots of the interaction of an lithotripter shock wave with a cylindrical shaped stone. The snap-shots show the distribution of the maximum tensile stress inside the stone at each instant of time. In the first two frames the shock wave can be seen to enter the stone as compressional waves. The third and fourth frames show that the longitudinal wave inside the stone and the acoustic wave outside the stone result in the generation of shear waves from the lateral walls. Further, between the third and fourth frames the shock wave reflects from the rear wall. Because the impedance of the surrounding fluid is less than that of the stone the reflected pressure wave is inverted and the leading compressive wave is reflected as a tensile wave. This is because the pressure reflection coefficient R_P given in Eq. 38-19 is negative if $Z_2 < Z_1$. The last two frames show the shear and longitudinal waves interfere to produce the high tensile stresses in the stone.

Acoustic Properties of Stones The most important material properties of kidney stones from the point of view of wave propagation are (1) density ρ_0, (2) longitudinal sound-speed c_L, and (3) transverse wave velocity c_T. Figure 38-17 shows reported measurements from human stones.[56–58] There is a large variation in the reported properties for uric acid, calcium oxylate monohydrate and cystine stones, for example, the sound speed in calcium oxylate monohydrate varies between 3,000 m/s and 4,500 m/s. This variation is likely due to the natural variation in the properties of the stones but may also be related to the preparation of the stones (eg, the amount of hydration).

How Shock Waves Break Stones Numerous mechanisms by which shock waves may fragment stones have been described in the literature. Here, we give a synopsis of some of the most likely mechanisms (Figure 38-18).

Spall Fracture *Spallation* occurs after the shock wave enters the stone and subsequently reflects from the rear of the stone (see Figure 38-16). The stone/urine interface inverts the large positive pressure pulse, resulting in a large tensile stress. This stress is added to the tensile stress of the still-incoming negative pressure tail, resulting in a very large tensile stress near the back wall.[59–62] Most solids are much weaker in tension than in compression, and so the large tensile stress near the rear of the stone can be expected to make the material fail.

Shear Stress *Shear* stresses will be generated by a combination of both shear waves and compressive waves that develop as the shock wave passes into the stone (Figure 38-19).[55,63] Many materials are weak in shear, particularly like kidney stones if they consist of layers, as the bonding strength of the matrix between layers often has a low ultimate shear stress.[59,60,64,65] Furthermore, the organic binder of kidney stones is much softer than the crystalline phase, and as the shock front passes through the stone, it will induce very large shear stresses at the binder/crystal interfaces, which likely contribute to the fracture of the kidney stone.[55,66] Shear waves in the stone can also result in large tensile stresses that exceed the tensile stress induced by spallation.[55] In Fig 38-16 it was shown that shear waves interfere with the reflected longitudinal wall to produce the largest tensile stress in the cylindrical stone.

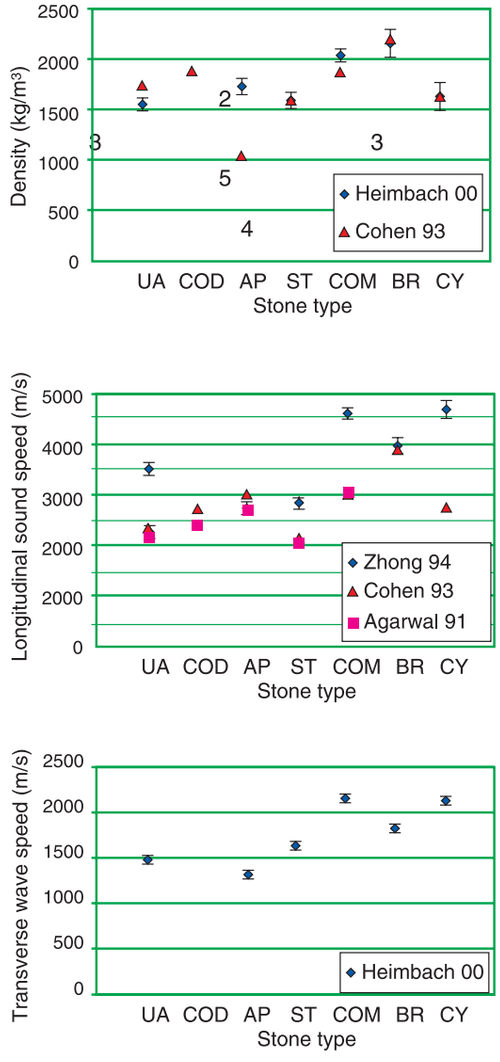

Figure 38-17 Reported measurements of acoustic properties in human stones. Top: density; Middle: sound speed; Bottom: shear wave speed. (UA = uric acid; COD = calcium oxylate dihydrate; AP = Apatite; ST = Struvite; COM = calcium oxylate monohydrate; BR = brushite; CY = cystine). Adapted from Agarwal R, Singh VR,[56] Cohen NP, Whitfield HN,[57] and Zhong P, Preminger GM.[58]

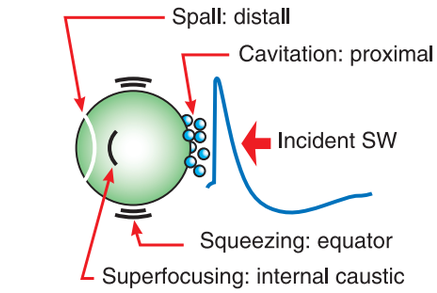

Figure 38-18 Schematic showing regions where different stone fracture mechanisms will act.

Superfocusing *Superfocusing* is the amplification of stresses inside the stone due to the geometry of the stone. The shock wave that is reflected at the distal surface of the stone can be focused either by refraction (associated with the high sound-speed and geometry of the stone) or by diffraction from the corners of the stone. It has been shown that these reflected waves can be focused to caustics (regions of high stress) in the interior of the stone and that this can lead to failure.[65,67] The regions of high stress (both tensile and shear) can be determined from the geometry of the stone and its elastic properties (eg, density, longitudinal wave speed, and shear wave speed).

Squeezing *Squeezing/splitting* occurs because of the difference in sound speed between

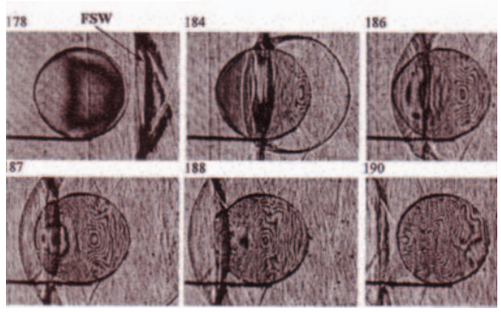

Figure 38-19 Images of the stress waves in a cylindrical stone (14 mm diameter), which was subject to a shock wave from a Dornier HM3. At 178 μs, the shock wave is almost incident on the stone. At 184 μs, the shock wave has entered the stone and has also reflected. At 186 μs, the compressive phase of the shock wave has just made it to the distal surface of the stone, and a shear wave can be seen at the midpoint of the stone. At 187 μs, the compressive wave has exited the stone, and the shear wave is focused along the axis of the stone. At 188 μs, the shear wave reaches the distal surface of the stone. At 190 μs, the shock wave has passed by the stone but stress waves are still reverberating inside the stone. (Images courtesy of Dr. P. Zhong—Figure 9a of [65]).

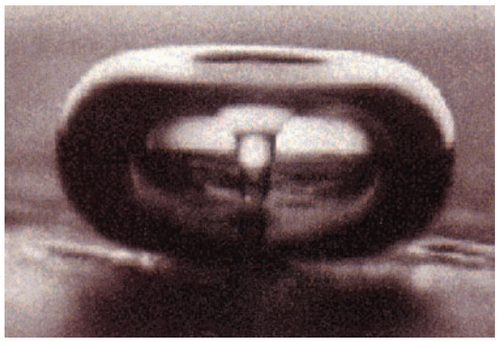

Figure 38-20 Image of a cavitation bubble collapsing on a metal surface. A jet of fluid can be seen punching through the center of the bubble toward the metal surface. Reproduced with permission from Crum LA.[27]

the stone (greater than 2,500 m/s) and the surrounding fluid (≈1,500 m/s). The shock wave inside the stone "runs away" from the shock wave propagating through the fluid outside of the stone (see Figure 38-16C and Figure 38-16D). The shock wave that propagates in the fluid outside the stone results in a circumferential force on the stone (known as a hoop stress). This results in a maximum tensile stress at proximal and distal ends of the stone and leads to an axial "splitting" failure. It has been theorized that squeezing should be enhanced when the entire stone falls within the diameter of the focal zone, and a lithotriptor based on this principal has recently been built and described in the literature.[68,69]

Cavitation *Cavitation* refers to small bubbles (or cavities) that grow in the urine surrounding the stone in response to the large negative pressure tail of the acoustic pulse. When a cavitation bubble collapses near a solid surface (eg, a kidney stone) a microjet of fluid is formed that pierces the bubble and impacts the surface (Figure 38-20) with speeds upwards of 100 m/s.[27] This jet likely plays a role in cavitation-induced damage to kidney stones.[27,28] The collapse of the cavitation bubble also results in the emissions of secondary shock waves that are radiated into the bubble. These secondary shock waves have an amplitude comparable to that of the focused shock wave. In vitro experiments where cavitation is suppressed show significant reduction in stone fragmentation.[43,70,71] Cavitation is principally a surface-acting mechanism, and experiments indicate that it acts most strongly on the proximal (shock wave incident) surface of the stone.[28,61,72] It has also been suggested that the stresses imparted by cavitation can act by a spall mechanism.[67,73] Recent work has recognized that the cavitation generated by lithotriptors acts as a cluster of bubbles (Figure 38-21) rather than individual bubbles, and that the coherent collapse of the cluster may enhance the destructive power of cavitation.[36,74,75]

Fatigue *Fatigue* is a process that may occur anywhere in the stone. Its hallmark is the progressive development of cracks.[76,77] The cracks are nucleated at sites of small imperfections that occur in almost all materials—these nucleation sites will be present in all kidney stones. The imperfections are sites of "stress concentrations" which, when a shock wave passes, can lead to local stresses far in excess of the average stress induced by the shock wave. With the impact of repetitive shock waves, the imperfections frow into microcracks. With subsequent shock waves, the microcracks grow into macrocracks, and eventually produce cracks large enough to induce failure. The cracks can be grown either by large tensile stresses or by large shear stresses. Therefore, fatigue will be enhanced wherever regions of high stress coincide with weak points in the stone. This means that there could be a synergistic effect between fatigue and some of the other mechanisms that result in localized regions of high tensile or shear stress. There are two pieces of evidence that strongly support the argument that stone comminution is a fatigue process. First, the internal structure of stones has been shown to affect how they fragment in lithotripsy.[55,78–80] Second, normally more than 1,000 shock waves are required to progressively fragment stones into sufficiently small pieces; the use of multiple stress cycles to fracture a material is a classic hallmark of fatigue.[76,77]

Although, present understanding of shock wave lithotripsy indicates that the stones fail through a fatigue process, it is not clear which mechanism drives the fatigue. The two most commonly cited mechanisms are direct stresses (spall and shear) and cavitation or some combination of them.[81] Part of the problem in determining which mechanism is that only limited data on the material strength of kidney stones have been reported (eg, ultimate strength in compression, fracture toughness, Knoop hardness, and Vickers microhardness.[56–58,82–85]) Of note is the paucity of data for the tensile and shear strength of kidney stones. This is most likely because determining these properties in brittle materials is fraught with technical difficulties. Further, most of the data have been measured in quasi-static tests, with the stress applied over many minutes, and the results may not be representative of the material properties when subject to shock waves, where the stress is applied and removed in microseconds.[66] At present, the data on material strength of kidney stones is not sufficient for the fracture process to be described.

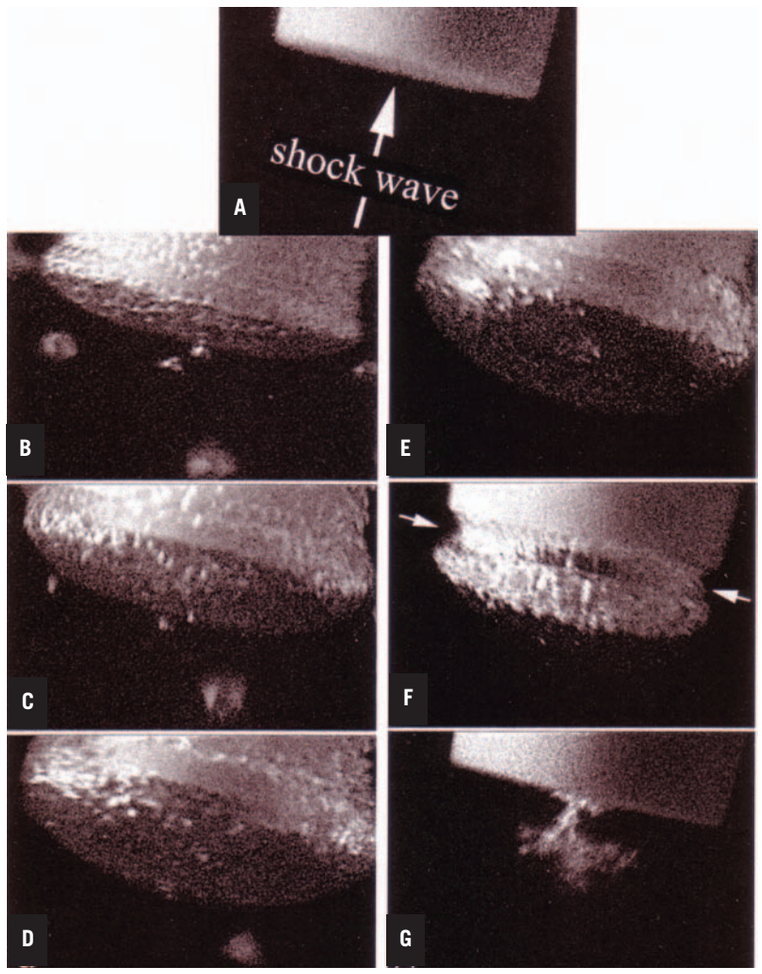

Figure 38-21 Images of cavitation bubble cluster collapse on a model stone 6.5 mm in diameter and 7.5 mm long. *A*, Orientation of shock wave to stone. *B*, 100 μs after shock wave arrival, a bubble cluster has formed on the proximal surface and a few bubbles have formed in the surrounding fluid. *C to E*, (200, 300 and 400 μs after shock wave arrival) the cluster continues to grow. *F*, The cluster begins to collapse in a mushroom like shape. *G*, The final collapse of the cluster at the center of the stone. Reproduced with permission from Pishchalnikov YA, et al.[36]

Mechanisms of Tissue Damage It is now well recognized that SWL results in trauma to the kidney and that, in some cases, the injury can be severe.[6] The clinical implications of such adverse effects are still under investigation (see Chapter 41, "Complications").

The notion that lithotriptor shock waves can pass harmlessly through the body is simply not true. It is likely that all patients who receive at least an average dose of shock waves (2,000 shock waves at midrange power or higher) experience some form of tissue trauma. Lithotripsy has been very beneficial for a large number of patients but has also led to severe, even catastrophic, adverse effects for others.[86] To better understand how shock waves have the potential to cause tissue trauma, consider the physics of the problem.

As discussed above lithotriptors produce a focused acoustic pulse. The acoustic field is broad at the source and narrow at the focus. The focal zone, the area of highest acoustic pressure, is elongated and of dimensions that cannot be localized exclusively to a stone. Although shock waves are targeted onto the stone, the surrounding tissue is also subject to significant mechanical forces. We have seen that the length of the focal zone of most lithotriptors is about 50 mm (see Figure 38-15), and this means that the entire thickness of the kidney is subject to high amplitude shock waves. In addition, patient motion, due to respiration or discomfort, likely results in the stone spending a good portion of the treatment time out of the focal region, and thus, many of the shock waves will interact solely with tissue.

Fortunately, tissue has physical properties that make it far less susceptible to damage by shock waves than kidney stones. For example, the fact that the acoustic impedance of tissue is close to that of water means that shock waves can pass through a tissue-to-water interface without significant reflection. Thus, tissue is not subjected to the extreme tensile forces that cause stones to fail by spallation. Further, the sound speed in tissue is almost constant, and so tissue will not be under a differential squeezing stress that could result in splitting. Tissue is, however, subject to shear forces induced by the pressure wave and to cavitation induced by the tensile phase of the shock wave. We will briefly describe the mechanisms that may contribute to tissue injury.

Mechanical Stress The positive pressure of a lithotriptor pulse leads to significant compression of tissue. Although tissue is usually robust to isotropic compression, the leading shock front has a rise time of the order of 70 ns in tissue which corresponds to a spatial scale of 100 μm. Therefore, tissue structures in the range of 10 μm to 1 mm will experience a significant variation in stress across them as the shock wave passes. The short rise time associated with the shock will lead to non-uniform straining of the tissue, resulting in shear forces. It is generally recognized that tissue structures are sensitive to shear stress, and the distortion of the tissue by the shock wave could induce enough shear to cause damage.[87,88]

Shear Induced by Inhomogeneities Tissue is an inhomogeneous medium at multiple length scales. Spatial variation in the sound speed on the millimeter length scale can have a dramatic effect on the focusing of ultrasonic pulses in tissue.[89] As the shock wave focuses, parts of the wavefront that passed through tissue with high sound speed will be advanced, and the parts that passed though low sound speed tissue will fall back. This distortion in the wavefront will lead directly to shear stresses in the tissue. Again these shear stresses could be strong enough to induce mechanical damage of the tissue.[87]

Cavitation Cavitation is known to occur in tissue during lithotripsy.[35,90,91] Measurements using passive cavitation detection in both humans and pigs have detected the unique acoustic signature associated with cavitation. Measurements have indicated the presence of cavitation in the perirenal fat, the collecting system, the parenchyma, and in subcapsular hematomas. Cavitation has been well documented to have a significant biological effect in many in vitro settings (see Carstensen EL, et al,[92] Miller DL and Thomas RM,[93] Miller M, et al,[94] Dalecki D, et al,[95] Delius M, et al,[96] and Williams JC, et al[97]). Experiments in lithotripsy indicate that damage to in vitro cells and in vivo tissue is dramatically reduced when cavitation is reduced or eliminated.[97–99] Cavitation is most likely the dominant cause of damage in tissue.

Cavitation is more likely to result in injury within blood vessels than within the surrounding tissue. This is because a bubble surrounded by tissue will be constrained and will not be able to go through a violent growth-and-collapse cycle. In a blood vessel, there is a fluid environment for the bubbles to grow and collapse. There are at least two mechanisms by which bubbles could produce mechanical damage to organs such as the kidney:

Collapsing Bubbles When cavitation bubbles collapse asymmetrically, they form high-velocity microjets of fluid focused to a small spot. These liquid microjets, forceful enough to pit foils or etch metal surfaces, seem easily capable of puncturing the fragile wall of a capillary or other blood vessel. Thus, just as cavitation bubble cluster collapse is believed to contribute to the breakage of stones, bubble collapse may play a role in the rupture of vessels. The weakness of this argument is that the blood vessels that are injured during lithotripsy typically are not large enough to allow cavitation bubbles to undergo a complete growth-collapse cycle.

Bubble Expansion Bubbles may rupture vessel walls during the expansion phase of the bubble cycle. That is, as the negative pressure of the shock wave passes through the vessel, it causes the bubble to undergo explosive growth (see Figure 38-10) pushing outward on the vessel and rupturing it. This is consistent with the observation that damage occurs first in the capillaries, which, due to their small size, will be subject to greater stresses during the most explosive part of the growth cycle. Experiments using capillary phantoms in an in vitro setting support the explosive bubble hypothesis.[100,101] This mechanism may also allow for other tissue to be damaged, for, if bubble growth is capable of rupturing vessels, it may be able to rip apart other tissue structures in the vicinity as well.

Once blood vessels have been ruptured and blood has collected in pools, in a hematoma for example, there is a greater potential for cavitation to occur. The pooling of blood provides a large fluid-filled space for cavitation bubbles to grow and collapse. Also, existing bubbles, which can act as nuclei for subsequent cavitation events, will not be swept away by blood flow, but will remain in the pooled region. This explains the intense PCD cavitation signals and B-scan ultrasound echogenicity collected from hematomas during SWL.[90,91,102] The violent cavitation in such a region could lead to further disruption of cells in the area.

Research continues in this area, with the goal of confirming whether the physical processes outlined here, or some other processes, are responsible for tissue damage in shock wave lithotripsy. This is partly due to the fact that the mechanical response of the tissue, at least at strain rates relevant in shock wave lithotripsy, is not well understood and so damage criteria are also not well defined. Further, there are few experimental systems that can be used to test and validate different hypotheses. Although the general consensus among researchers is that cavitation is the primary mechanism for tissue injury, this field still requires much study.

The Evolution of the Lithotriptor **How Lithotriptors Have Changed Over the Years** It is more than 25 years since the introduction of lithotripsy to clinical practice, and there have been a number of noteworthy changes in equipment design, but none that have involved a fundamental change in the acoustics of the lithotriptor. That is, lithotriptors have changed—they are now compact, modular, use dry shock heads, have improved imaging—but the acoustic signature of the lithotriptor pressure pulse remains remarkably similar. The focal waveform generated by a Dornier HM3 is virtually the same as the waveform produced by any of the numerous lithotriptors available on the market today. This is not to imply that the lithotriptor industry has been static. Indeed, there has been a very active effort on the part of manufacturers to produce machines that are easier and more practical to use. In this regard, lithotripsy has seen numerous refinements. At the same time, however, it is essential to note that success rates in lithotripsy have declined. The use of newer lithotriptors, specifically those that produce a tight focal zone of extreme peak positive pressure, has led to decreased efficiency of stone breakage and to an increase in collateral damage.[2] Thus, progress in lithotripsy has taken a step back—improved convenience has been gained, but at a cost.

The first lithotriptors were electrohydraulic devices in which the shock wave was generated by underwater spark discharge, and shock wave coupling was achieved by immersion of the patient in a water bath. The Dornier HM3 was a

very popular lithotriptor of this era, and at some centers is still in use today. By today's standards, the Dornier HM3 produces moderate peak positive pressures (≈ 40 MPa) delivered to a generous focal zone (≈ 15 by 60 mm). The Dornier HM3 was a very successful machine, and it is probably safe to say that the early success and rapid acceptance of lithotripsy was built on the back of this particular lithotriptor.

Even though the Dornier HM3 was a very effective lithotriptor, it was perceived by some to have several significant drawbacks. It used an open water bath to couple shock waves to the body, treatment was painful, requiring the patient to be sedated (or even anaesthetized), and the lithotriptor was a large, stationary piece of equipment that required a dedicated water treatment plant. What physicians (and patients) really wanted was lithotripsy that was painless and convenient, with minimal to no anesthesia—a fully ambulatory walk-in/walk-out therapy. Lithotriptor manufacturers responded with a number of modifications. Problems related to the overall physical design of the lithotriptor were challenging but solvable. For example, the issue of the open water bath was addressed by enclosing the shock head and by using a rubber membrane to couple the shock wave to the body. This was not a perfect solution, as there is no better way to achieve acoustic coupling than through a water-tissue interface. Elimination of the water bath, however, meant that medical staff had much easier access to the patient, the lithotriptor did not necessarily have to be tied down to a dedicated facility, and that lithotriptors could be designed as modular systems. Many modern lithotriptors have indeed been designed to be portable and are used in mobile lithotripsy units.

Another perceived disadvantage of the Dornier HM3 was the limited life span of the electrodes. It is necessary to replace the electrode one or more times during a treatment. Electromagnetic and piezoelectric lithotriptors do not use electrodes, which is an advantage in terms of cost, time, and convenience. In addition to the need to periodically change electrodes, electrode wear is an issue with electrohydraulic lithotriptors. As the spark gap widens with use, there is increased variability in the path of the arc discharge. Several manufacturers of current electrohydraulic machines have found various ways to improve electrode life, and some use designs such as encapsulation in an electrolyte-filled housing to extend the life of the electrode.[103,104]

The attempt to design a lithotriptor so that it can be operated "anesthesia-free," on the other hand, has proven to be a much more difficult problem. Discomfort during shock wave treatment is due primarily to the sensation of cutaneous pain over the area of shock wave entry at the surface of the body. One attempted solution was to widen the aperture at the shock source in order to spread the energy over a broader area. A wider aperture broadens the acoustic field along the shock wave axis, but it narrows the focal zone of the pressure pulse. Many current lithotriptors have a very narrow focal zone (on the order of 5 mm or less). Some of these lithotriptors also generate huge peak positive pressures (in excess of 100 MPa). Use of a tight focal zone might prove to be an advantage if it could be kept directly on target, but it cannot. Because of respiratory motion, shooting at a stone using a narrow focal zone proves to be harder than when using a broad focal zone. Further, regardless of which lithotriptor is used, lithotripsy is uncomfortable for the patient. If the patient is not sedated he or she will move to try to get more comfortable. Thus, attempts to build a totally anesthesia-free device have not yet been successful.

Future Directions in Lithotriptor Design

There have been recent developments in lithotripsy that could herald a positive change for the future of SWL. That is, there has been an effort to introduce novel approaches in lithotriptor design that build upon well-tested theory—and positive experimental results—targeting ways to improve stone breakage and reduce tissue injury. One approach is a response to the recent trend toward tight–focal-zone, high–acoustic-pressure machines. The Xi Xin-Eisenmenger lithotriptor[69] is a wide-focus and low-pressure lithotriptor that generates the largest focal zone (18 by 180 mm) and lowest range of acoustic pressures (10 to 25 MPa) currently in use in clinical practice. This machine was developed to test the hypothesis that a very broad focal zone could be used to enhance stone breakage by circumferential squeezing.[68] It was reported in an early trial that this machine delivered a high stone-free rate (86%) and can be used anesthesia-free.[69]

Cavitation control may be a means to improve lithotripsy. The cavitation bubble cycle—the time for a bubble to grow and then collapse—lasts on the order of 300 μs in the free field and ≈ 600 μs at the surface of a stone.[105] Recent studies have shown that cavitation bubbles generated by one lithotriptor pulse can be manipulated by a second pulse.[106,107] If the second pulse arrives while bubbles are in their early growth phase, further expansion is stopped and the bubbles collapse with minimal damage. If, however, the second pulse arrives later in the cycle, bubble collapse is accelerated and damage is enhanced. Thus, the timing of the two pulses is critical. Bailey originated dual pulse lithotripsy, and in his studies used twin shock sources oriented coaxially facing one another.[108] Others have built upon this concept and developed lithotriptors that fire multiple pulses along the same axis[109–111] or machines that use dual treatment heads offset at an angle to accommodate the constraints imposed by the anatomy of a patient.[112–114] At the time of writing, dual pulse lithotripsy is under development and testing. The concept holds promise, as this may be a means to tailor acoustic forces within the focal zone for better breakage of stones, hopefully with reduced collateral damage. But it is too early to endorse such machines as there are, as yet, no data that assess these lithotriptors for efficacy and safety compared to conventional lithotriptors.

The safety of lithotripsy is a very important issue. Shock waves cause trauma, and any strategy that results in lowering the dose of shock waves needed to treat a patient should be welcomed. One way to reduce unnecessary shock wave impact on tissue is to track the stone during treatment and only fire when the shock wave will hit the stone. Devices have been proposed that would monitor stone location and only allow shock waves to be fired when the stone is at the focus of the lithotriptor.[115–118] A device has also been proposed to exploit acoustic time-reversal to dynamically change the focus of the lithotriptor and so hit the stone even as it moves.[119,120] Such concepts have the potential to dramatically reduce the number of shock waves required to break a stone. However, clinical devices do not currently employ real-time tracking.

SUMMARY

Shock wave lithotripsy is a superb example of the successful transition of engineering technology into the clinical area. We have outlined the underlying acoustic principles that describe (1) the generation of the shock pulse, (2) focusing, (3) nonlinear distortion, (4) coupling of the shock source to the body, and (5) absorption of sound by the body. The exact mechanisms by which shock waves can damage stones and tissue are still not fully understood, although it is likely that direct stresses and cavitation are dominant in stone fragmentation, and that cavitation is dominant in tissue injury. Improvements in lithotripsy, whether through improved use of existing lithotriptors or through the development of new technologies, are likely to come only from an improved understanding of the acoustics and the physics of this problem.

In this chapter we have attempted to make the following main points.

- Most lithotriptors produce a similar type of shock wave, which consists of a leading positive pressure shock front (compressive wave) lasting about 1 μs followed by a negative pressure trough (tensile wave), which lasts about 3 μs. There is a large range in the amplitude of the shock waves used, with peak positive pressures of 30 to 110 MPa depending on the type of shock source and the power setting.
- The intense compressive wave induces mechanical forces inside the stone that may lead to fragmentation, most likely by a spall mechanism. The tensile component of the shock wave is lower amplitude (about –8 to –15 MPa). This negative pressure drives cavitation bubble activity that is critical to stone comminution, but also causes vascular trauma to the kidney.
- Various types of shock wave sources and focusing mechanisms have been exploited in lithotripsy. Electromagnetic and electrohydraulic lithotriptors dominate the lithotripsy market today.
- The size and dimensions of the focal zone are controlled by diffraction. Typically, electro-

magnetic lithotriptors have a smaller focal zone than electrohydraulic devices and generate substantially higher peak positive pressures. A smaller focal zone is not necessarily an advantage because patient motion means that the stone can easily spend a significant amount of time outside the focal region. Currently, there is no good metric to determine equivalent action of different types of machines.

- Shock waves are coupled into the body using a water path that, ideally, is devoid of bubbles. Most current lithotriptors use an enclosed water path in which the shock head is capped by a rubber membrane of low acoustic impedance. Such dry lithotriptors tend not to be as efficient as the older water-bath lithotriptors in which the patient is immersed in water during treatment—and this reduced efficiency could be due, at least in part, to poorer coupling.
- The acoustic waveforms measured in vitro and in vivo are very similar, despite the presence of absorption and heterogeneity in tissue. This is a significant finding for it validates in vitro experimentation as being representative of the in vivo condition.
- Numerous mechanisms have been proposed to explain how shock waves break urinary stones. No single mechanism gives an adequate explanation, and it appears that multiple mechanisms involving cavitation and spallation are at play. For tissue injury on the other hand it appears that cavitation, and shock wave/bubble interaction, are the most likely cause of trauma.
- Since its inception, lithotripsy has undergone a fascinating evolution. Water bath-type, electrohydraulic devices have given way to modular, highly portable lithotriptors, many of which employ electromagnetic shock wave generators. Most lithotripsies are now performed using mobile units delivered by truck to subscribing hospitals. This improved convenience has come at a price as stone re-treatment rates have increased and reports of collateral damage are on the rise. One explanation is that the newer lithotriptors are not as efficacious and have the potential to cause more collateral damage.
- New technologies of shock wave delivery are now being applied to patient treatment. Dual-pulse lithotripsy uses two shock heads to fire separate pulses. In theory, it should be possible to treat patients faster, and the potential for control over the properties of the acoustic field could lead to improved efficacy and safety. Likewise, initial success with a new lithotriptor that produces a very broad focal zone and is operated at low peak positive pressures suggests that a return to some of the features of the original lithotriptor could also be a step toward improved lithotripsy.

ACKNOWLEDGEMENTS

We would like to thank Drs. Michael Bailey, Andrew Evan, James Lingeman, Yura Pishchalnikov, David Wang and James Williams Jr for their comments on this chapter. This research was supported in part by grants from the National Institutes of Health (NIH DK43881, DK55674) and the Whitaker Foundation (RG-01-0084).

REFERENCES

1. Holmes S, Whitfield HN. The current status of lithotripsy. Br J Urol 1991;68:337–44.
2. Kerbl K, Rehman J, Landman J, et al. Current management of urolithisasis: progress or regress? J Endourol 2002;16: 281–8.
3. Kohrmann KU, Rassweiler JJ, Manning M, et al. The clinical introduction of a 3rd generation lithotriptor - Modulith Sl-20. J Urol 1995;153:1379–83.
4. Lingeman JE, Newmark J. Adverse bioeffects of shock-wave lithotripsy. In: Coe FL, et al, editors. Kidney stones: medical and surgical management,. Philadelphia: Lippincott-Raven; 1996. p. 605–14.
5. Janetschek G, Frauscher F, Knapp R, et al. New onset hypertension after extracorporeal shock wave lithotripsy: age related incidence and prediction by intrarenal resistive index [see comments]. J Urol 1997;158:346–51.
6. Evan AP, Willis LR, Lingeman JE, McAteer JA. Renal trauma and the risk of long-term complications in shock wave lithotripsy. Nephron 1998;78:1–8.
7. Tan EC, Tung KH, Foo KT. Comparative studies of extracorporeal shock wave lithotripsy by Dornier HM3, EDAP LT 01 and Sonolith 2000 devices. J Urol 1991;148: 294–97.
8. Ueda S, Matsuko K, Yamashita T, et al., Perirenal hematomas caused by SWL with EDAP LT-01 lithotriptor. J Endourol 1993;7:11–15.
9. Fuselier HA, Prats L, Fontenot C, Gauthier A. Comparison of mobile lithotriptors at one institution: Healthtronics Lithotron, Dornier MFL-5000, and Dornier Doli. J Endourol 1999;13: 539–42.
10. IEC61846, Ultrasonics - Pressure pulse lithotriptors - Characteristics of fields, T.-. Ultrasonics, Editor. 1998.
11. Dreyer T, Riedlinger RE, Steiger E. Experiments on the relation of shock wave parameters to stone disintegration. 16th International Congress on Acoustics 1998. Seattle, WA, USA: Acoustical Society of America.
12. Averkiou MA, Cleveland RO. Modeling of an electrohydraulic lithotriptor with the KZK equation. J Acoust Soc Am 1999;106:102–12.
13. Fry FJ, Dins KA, R. C.R., G. S.A. Losses in tissue associated with finite amplitude ultrasound transmission. Ultrasound Med Biol 1989;15:481–97.
14. Hynynen K. The role of nonlinear ultrasound propagation during hyperthermia treatments. Med Phys 1991;18: 1156–63.
15. Averkiou MA, Hamilton MF. Nonlinear distortion of short pulses radiated by plane and focused circular pistons. J Acoust Soc Am 1997;102:2539–48.
16. Ward B, Baker AC, Humphrey VF. Nonlinear propagation applied to the improvement of resolution in diagnostic medical ultrasound. J Acoust Soc Am 1997;101:143–54.
17. Christopher T. Finite amplitude distortion-based inhomogeneous pulse echo ultrasonic imaging. IEEE Trans Ultrason Ferroelectr Freq Control 1997;44:125–39.
18. ter Haar G. Ultrasound focal beam surgery. Ultrasound Med Biol 1995;21:1089–100.
19. Hynynen K. Review of ultrasound therapy. In: 1997 IEEE Ultrasonics Symposium Proceedings: An International Symposium; 1997; Toronto, Canada. New York: IEEE.
20. Arefiev A, Prat F, Chapelon JY, et al. Ultrasound-induced tissue ablation: studies on isolated, perfused porcine liver. Ultrasound Med Biol 1998;24:1033–43.
21. Bailey MR, Khokhlova VA, Sapozhnikov OA, et al. Physical mechanisms of the therapeutic effect of ultrasound (a review). Acoustical Physics 2003;49:369–88.
22. Coleman AJ, Saunders JE, Preston RC, Bacon DR. Pressure waveforms generated by a Dornier extracorporeal shockwave lithotriptor. Ultrasound Med Biol 1987;13: 651–57.
23. Campbell DS, Flynn HG, Blackstock DT, et al. The acoustic fields of the Wolf electrohydraulic lithotriptor. J Lithotr Stone Dis 1991;3:147–56.
24. Staudenraus J, Eisenmenger W. Fibre-optic probe hydrophone for ultrasonic and shock-wave measurements in water. Ultrasonics 1993; 31:267–73.
25. Cleveland RO, Lifshitz DA, Connors BA, et al. In vivo pressure measurements of lithotripsy shock waves in pigs. Ultrasound Med Biol 1998;24:293–306.
26. Coleman AJ, Saunders JE, Crum LA, Dyson M. Acoustic cavitation generated by an extracorporeal shockwave lithotriptor. Ultrasound Med Biol 1987;13:69–76.
27. Crum LA. Cavitation microjets as a contributory mechanism for renal calculi disintegration in ESWL. J Urol 1988; 140:1587–90.
28. Delius M, Brendel W, Heine G. A mechanism of gallstone destruction by extracorporeal shock waves. Naturwissenschaften 1988;75:200–1.
29. Atchley AA, Prosperetti A. The crevice model of bubble nucleation. J Acoust Soc Am 1989;86(3):1065–84.
30. Church C. A theoretical study of cavitation generated by an extracorporeal shock wave lithotriptor. J Acoust Soc Am 1989;86:215–27.
31. Matula TJ, Hilmo PR, Storey BD, Szeri AJ. Radial response of individual bubbles subjected to shock wave lithotripsy pulses in vitro. Phys Fluids 2002;14(3):913–21.
32. Coleman AJ, Choi MJ, Saunders JE, Leighton TG. Acoustic emission and sonoluminescence due to cavitation at the beam focus of an electrohydraulic shock wave lithotriptor. Ultrasound Med Biol 1992;18:267–81.
33. Philipp A, Delius M, Scheffczyk C, et al. Interaction of lithotriptor-generated shock waves with air bubbles. J Acoust Soc Am 1993;93:2496–509.
34. Sass W, Matura E, Dreyer HP, et al. Lithotripsy-mechanisms of the fragmentation process with focussed shock waves. Electromedica 1993;61:2–12.
35. Zhong P, Cioanta I, Cocks FH, Preminger GM. Inertial cavitation and associated acoustic emission produced during electrohydraulic shock wave lithotripsy. J Acoust Soc Am 1997;101:2940–50.
36. Pishchalnikov YA, Sapozhnikov OA, Bailey MR, et al. Cavitation bubble cluster activity in the breakage of kidney stones by lithotriptor shockwaves. J Endourol 2003;17:435–46.
37. Matula TJ, Hilmo PR, Bailey MR, Crum LA. In vitro sonoluminescence and sonochemistry studies with an electrohydraulic shock-wave lithotriptor. Ultrasound Med Biol 2002;28:1199–207.
38. Coakley W. Acoustical detection of single cavitation events in a focused field in water at 1 MHz. J Acoust Soc Am 1971; 49:792–801.
39. Roy RA, Madanshetty SI, Apfel RE. An acoustic backscattering technique for the detection of transient cavitation produced by microsecond pulses of ultrasound. J Acoust Soc Am 1990;87:2451–8.
40. Madanshetty SI, Roy RA, Apfel RE. Acoustic microcavitation: its active and passive acoustic detection. J Acoust Soc Am 1991;90:1515–26.
41. Cleveland RO, Sapozhnikov OA, Bailey MR, Crum LA. A dual passive cavitation detector for localized detection of lithotripsy-induced cavitation in vitro. J Acoust Soc Am 2000;107:1745–58.
42. Coleman AJ, Whitlock M, Leighton T, Saunders JE. The spatial distribution of cavitation induced acoustic emission, sonoluminescence and cell lysis in the field of a shock wave lithotriptor. Phys Med Biol 1993;38:1545–60.
43. Bailey MR, Blackstock DT, Cleveland RO, Crum LA. Comparison of electrohydraulic lithotriptors with rigid and pressure-release ellipsoidal reflectors. II. Cavitation fields. J Acoust Soc Am 1999;106:1149–60.
44. Lifshitz DA, Williams JC Jr, Sturtevant B, et al. Quantitation of shock wave cavitation damage in vitro. Ultrasound Med Biol 1997;23:461–71.
45. Pye SD, Dineley JA. Characterization of cavitational activity in lithotripsy fields using a robust electromagnetic probe. Ultrasound Med Biol 1999;25:451–71.
46. Church CC, Crum LA. A theoretical study of cavitation generated by four commercially available extracorporeal shock wave lithotriptors. In: Frontiers of Nonlinear Acoustics: Proceedings of 12th ISNA; 1990; Austin (TX). New York: Elsevier.
47. Cartledge JJ, Cross WR, Lloyd SN, Joyce AD. The efficacy of a range of contact media as coupling agents in extracorporeal shockwave lithotripsy. BJU Int 2001;88:321–4.
48. Coleman AJ, Saunders JE. A survey of the acoustic output of commercial extracorporeal shock wave lithotriptors. Ultrasound Med Biol 1989;15:213–27.
49. Buizza A, Dell'Aquila T, Giribona P, Spagno C. The performance of different pressure pulse generators for extracorporeal lithotripsy: a comparison based on commercial lithotriptors for kidney stones. Ultrasound Med Biol 1995;21:259–72.
50. Chuong CJ, Zhong P, Preminger GM. A comparison of stone damage caused by different modes of shock wave generation. J Urol 1992;148:200–5.
51. Teichman JMH, Portis AJ, Cecconi PP, et al. In vitro comparison of shock wave lithotripsy machines. J Urol 2000;164: 1259–64.

52. Cleveland RO, Anglade R, Babayan RK. Effect of stone motion on in vitro comminution efficiency of a Storx Modulith SLX. J Endourol 2004;18:629–33.
53. Chitnis PV. Characterization and comparative analysis of extracorporeal shock wave devices. In: Aerospace and mechanical engineering. Boston: Boston University; 2002. p. 108.
54. Paterson RF, Lifshitz DA, Lingeman JE, et al. Stone fragmentation during shock wave lithotripsy is improved by slowing the shock wave rate: studies with a new animal model. J Urol 2002;168:2211–15.
55. R.O Cleveland and O.A. Sapozhnikov. Modeling elastic wave propagation in kidney stones with application to shock wave lithotripsy. J Acoust Soc Am 2005;118:2667–76.
56. Agarwal R, Singh VR. A comparative study of fracture strength, ultrasonic properties and chemical constituents of kidney stones. Ultrasonics 1991;29:89–90.
57. Cohen NP, Whitfield HN. Mechanical testing of urinary calculi. World J Urol 1993;11:13–8.
58. Zhong P, Preminger GM. Mechanisms of differing stone fragility in extracorporeal shockwave lithotripsy. J Endourol 1994;8:263–68.
59. Chaussy C, Brendel W, Schmiedt E. Extracorporeally induced destruction of kidney stones by shock waves. Lancet 1980;2:1265–8.
60. Chaussy C. Extracorporeal shock wave lithotripsy: new aspects in the treatment of kidney stone disease. 1982. Basel, Switzerland: S Karager.
61. Sass W, Braunlich M, Dreyer H-P, et al. The mechanisms of stone disintegration by shock waves. Ultrasound Med Biol 1991;17:239–43.
62. Ding Z,. Gracewski SM. Response of constrained and unconstrained bubbles to lithotriptor shock wave pulses. J Acoust Soc Am 1994;96:3636–44.
63. Sapozhnikov OA, Cleveland RO, Bailey MR, Crum LA. Modeling of stresses generated by lithotriptor shock wave in cylindrical kidney stone. In: 3rd International Symposium of Therapeutic Ultrasound. 2004. Lyon, France.
64. Dahake G, Gracewski SM. Finite difference predictions of P-SV wave propagation inside submerged solids. II. Effect of geometry. J Acoust Soc Am 1997;102:2138–45.
65. Xi X, Zhong P. Dynamic photoelastic study of the transient stress field in solids during shock wave lithotripsy. J Acoust Soc Am 2001;109:1226–39.
66. Sylven ET, Agarwal S, Cleveland RO, Briant CL. High strain rate testing of kidney stones. J Mater Sci Mater Med 2004;15:613–17.
67. Gracewski SM, Dahake G, Ding Z, et al. Internal stress wave measurements in solids subjected to lithotriptor pulses. J Acoust Soc Am 1993;94:652–61.
68. Eisenmenger W. The mechanisms of stone fragmentation in ESWL. Ultrasound Med Biol 2001;27:683–93.
69. Eisenmenger W, Du XX, Tang C, et al. The first clinical results of "wide focus and low pressure" ESWL. Ultrasound Med Biol 2002;28:769–74.
70. Holmer NG, Almquist LO, Hertz TG, et al. On the mechanism of kidney-stone disintegration by acoustic shock-waves. Ultrasound Med Biol 1991;17:479–89.
71. Sapozhnikov OA, Khokhlova VA, Bailey MR, et al. Effect of overpressure and pulse repetition frequency on cavitation in shock wave lithotripsy. J Acoust Soc Am 2002; 112(3).
72. Delacretaz G, Rink K, Pittomvils G, et al. Importance of the implosion of ESWL-induced cavitation bubbles. Ultrasound Med Biol 1995; 21:97–103.
73. Zhong P, Chuong CJ, Preminger GM. Propagation of shock waves in elastic solids caused by cavitation microjet impact. II: Application in extracorporeal shock wave lithotripsy. J Acoust Soc Am 1993;94:29–36.
74. Pittomvils G, Lafaut JP, Vandeursen H, et al. Macroscopic ESWL-induced cavitation: in vitro studies. Ultrasound Med Biol 1995;21:393–8.
75. Tanguay M, Colonius T. Numerical investigation of bubble cloud dynamics in shock wave lithotripsy. In: 2002 ASME Fluids Engineering Division Summer Meeting. 2002.
76. Sturtevant B. Shock wave physics of lithotriptors. In: Smith AD, editor. Smith's textbook of endourology. St. Louis: Quality Medical Publishing, Inc.; 1996. p. 529–52.
77. Lokhandwalla M, Sturtevant B. Fracture mechanics model of stone comminution in ESWL and implications for tissue damage. Phys Med Biol 2000;45:1923–40.
78. Pittomvils G, Vandeursen H, Wevers M, et al. The influence of internal stone structure upon the fracture behaviour of urinary calculi. Ultrasound Med Biol 1994;20:803–810.
79. Cleveland RO, McAteer JA, and Muller R. Time-lapse nondestructive assessment of shock wave damage to kidney stones in vitro using micro-computed tomography. J Acoust Soc Am 2001;110:1733–6.
80. Williams JC Jr, Saw KC, Paterson RF, et al. Variability of renal stone fragility in shock wave lithotripsy. Urology 2003;61:1092–6.
81. Zhu S, Cocks FH, Preminger GM, Zhong P. The role of stress waves and cavitation in stone comminution in shock wave lithotripsy. Ultrasound Med Biol 2002;28:661–71.
82. Burns JR, Shoemaker BE, Gauthier JF, Finlayson B. Hardness testing of urinary calculi. In: Schwille PO, Others ETC, editors. Urolithiasis and related clinical research. New York: Plenum Press; 1985. p. 703–6.
83. Ebrahimi F, Wang F. Fracture behavior of urinary stones under compression. J Biomed Mater Res 1989;23:507–21.
84. Singh VR, Dhawan JB. Ultrasonic velocity and attenuation measurement in kidney stones: correlation to constituents and hardness. Biomed Mater Eng 1992;2:79–82.
85. Zhong P, Chuong CJ, Preminger GM. Characterization of fracture toughness of renal calculi using a microindentation technique. (Extracorporeal shock wave lithotripsy). J Mater Sci Lett 1993;12:1460–2.
86. Tuteja AK, Pulliam JP, Lehman TH, Elzinga LW. Anuric renal failure from massive bilateral renal hematoma following extracorporeal shock wave lithotripsy. Urology 1997;50: 606–8.
87. Lokhandwalla M, Sturtevant B. Mechanical haemolysis in shock wave lithotripsy (SWL). I. Analysis of cell deformation due to SWL flow-fields. Phys Med Biology 2001; 46:413–37.
88. Lokhandwalla H, McAteer JA, Williams JC Jr, Stuftevant B. Mechanical haemolysis in shock wave lithotripsy (SWL): II. In vitro cell lysis due to shear. Phys Med Bio 2001;46:1245–64.
89. Mast TD, Hinkelman LM, Metlay LA, et al. Simulation of ultrasonic pulse propagation, distortion, and attenuation in the human chest wall. J Acoust Soc Am 1999;106:3665–77.
90. Coleman AJ, Choi MJ, Saunders JE. Detection of acoustic emission from cavitation in tissue during clinical extracorporeal lithotripsy. Ultrasound Med Biol 1996;22: 1079–87.
91. Sapozhnikov OA, Bailey MR, Crum LA, et al. Ultrasound-guided localized detection of cavitation during lithotripsy in pig kidney in vivo. IEEE Ultrasonics Symposium 2001. p. 1347–50.
92. Carstensen EL, Child SZ, Crane C, et al. Lysis of cells in Elodea leaves by pulsed and continuous wave ultrasound. Ultrasound Med Biol 1990;16:167–73.
93. Miller DL, Thomas RM. Contrast-agent gas bodies enhance hemolysis induced by lithotriptor shock waves and high-intensity focused ultrasound in whole blood. Ultrasound Med Biol 1996;22:1089–95.
94. Miller M, Miller D, Brayman A. A review of in vitro bioeffects of intertial ultrasonic cavitation from a mechanistic perspective. Ultrasound Med Biol 1996;22:1131–54.
95. Dalecki D, Raeman CH, Child SZ, Carstensen EL. A test for cavitation as a mechanism for intestinal hemorrhage in mice exposed to a piezoelectric lithotripter. Ultrasound Med Biol 1996;22:493–6.
96. Delius M, Denk R, Berding C, et al. Biological effects of shock waves: cavitation by shock waves in piglet liver. Ultrasound Med Biol 1990;16:467–72.
97. Williams JC Jr, Woodward JF, Stonehill MA, et al. Cell damage by lithotriptor shock waves at high pressure to preclude cavitation. Ultrasound Med Biol 1999;25:1445–9.
98. Delius M. Minimal static excess pressure minimises the effect of extracorporeal shock waves on cells and reduces it on gallstones. Ultrasound Med Biol 1997;23:611–7.
99. Evan AP, Willis LR, McAteer JA, et al. Kidney damage and renal functional changes are minimized by waveform control that suppresses cavitation in shock wave lithotripsy. J Urol 2002;168:1556–62.
100. Zhong P, Cioanta J, Zhu S, et al. Effects of tissue constraint on shock wave-induced bubble expansion in vivo. J Acoust Soc Am 1998;104:3126–9.
101. Zhong P, Zhou Y, Zhu S. Dynamics of bubble oscillation in constrained media and mechanisms of vessel rupture in SWL. Ultrasound Med Biol 2001;27:119–34.
102. Kuwahara M, Ioritani N, Kambe K, et al. Hyperechoic region induced by focused shock waves in vitro and in vivo: possibility of acoustic cavitation bubbles. J Lithotr Stone Dis 1989;1:282–8.
103. Bourlion M, Dancer P, Lacoste F, et al. Design and characterization of a shock wave generator using canalized electrical discharge: application to lithotripsy. Rev Sci Instrum 1994;65:2356–63.
104. Cleveland R, Chitnis P, Gerbus B, McAteer J. An in vitro comparison of open-cage and encapsulated electrodes in shock wave lithotripsy (SWL). European Association of Urology. 2004.
105. Bailey MR, Cleveland RO, Williams JC Jr, et al. Effect of increased ambient pressure on lithotripsy-induced cavitation in bulk fluid and at solid surfaces. In: Joint Meeting of the Acoustical Society of America, European Acoustics Association and German Acoustics DAGA Conference. 1999. Berlin, Germany: Deutsche Gesellschaft fur Akustik (DEGA).
106. Sokolov DL, Bailey MR, Crum LA. Use of a dual-pulse lithotriptor to generate a localized and intensified cavitation field. J Acoust Soc Am 2001;110(3 Pt 1):1685–95.
107. Sokolov DL, Bailey MR, Crum LA. Dual-pulse lithotriptor accelerates stone fragmentation and reduces cell lysis in vitro. Ultrasound Med Biol 2003;29:1045–52.
108. Bailey MR. Control of acoustic cavitation with application to lithotripsy. J Acoust Soc Am 1997;102:1250–1250.
109. Prieto FE, Loske AM. Bifocal reflector for electrohydraulic lithotriptors. J Endourol 1999;13:65–75.
110. Huber P, Debus J, Jöchle K, et al. Control of cavitation activity by different shockwave pulsing regimes. Phys Med Biol 1999;44:1427–37.
111. Zhong P, Zhou YF. Suppression of large intraluminal bubble expansion in shock wave lithotripsy without compromising stone comminution: methodology and in vitro experiments. J Acoust Soc Am 2001;110:3283–91.
112. Zhong P, Cocks FH, Cionta I, Preminger GM. Controlled, forced collapse of cavitation bubbles for improved stone fragmentation during shock wave lithotripsy. J Urol 1997;158:2323–8.
113. Xi X, Zhong P. Improvement of stone fragmentation during shock-wave lithotripsy using a combined EH/PEAA shock-wave generator-in vitro experiments. Ultrasound Med Biol 2000;26:457–67.
114. Sheir KZ, El-Sheikh AM, Ghoneim MA. Synchronous twin-pulse technique to improve efficacy of SWL: Preliminary results of an experimental study. J Endourol 2001; 15:965–74.
115. Kuwahara MA, Kambe K, Taguchi K, et al. Initial experience using a new type extracorporeal lithotriptor with an anti-misshot control device. J Lithotr Stone Dis 1991;3:141–6.
116. Orkisz M, Farchtchian T, Saighi D, et al. Image based renal stone tracking to improve efficacy in extracorporeal lithotripsy. J Urol 1998;160:1237–40.
117. Chang CC, Liang SM, Pu YR, et al. In vitro study of ultrasound based real-time tracking of renal stones for shock wave lithotripsy: part I. J Urol 2001;166:28–32.
118. Chang CC, Manousakas I, Pu YR, et al. In vitro study of ultrasound based real-time tracking for renal stones in shock wave lithotripsy: Part II - A simulated animal experiment. J Urol 2002;167:2594–97.
119. Thomas J-L, Wu F, Fink M. Time reversal focusing applied to lithotripsy. Ultrason Imaging 1996;18:106–21.
120. Montaldo G, Roux P, Derode A, et al. Ultrasound shock wave generator with one-bit time reversal in a dispersive medium, application to lithotripsy. Appl Phys Lett 2002;80:897–9.